Stress Recovery Triggers Rapid Transcriptional Reprogramming and Activation of Immunity in Plants

Natanella Illouz-Eliaz[1,2], Jingting Yu[3], Joseph Swift[1,2], Kathryn Lande[3], Bruce Jow[2], Za Khai Tuang[4], Travis Lee[1,2,6], Adi Yaaran[5], Rosa Gomez Castanon[2], Joseph R. Nery[2], Tatsuya Nobori[1,2], Yotam Zait[5], Saul Burdman[4], and Joseph R. Ecker[1,2,4*]

[1]Plant Biology Laboratory, The Salk Institute for Biological Studies, La Jolla, CA 92037, United States
[2]Genomic Analysis Laboratory, The Salk Institute for Biological Studies, La Jolla, CA 92037, United States
[3]The Razavi Newman Integrative Genomics and Bioinformatics Core Facility, The Salk Institute for Biological Studies, La Jolla, CA92037, United States
[4]Department of Plant Pathology and Microbiology, Institute of Environmental Sciences, The Robert H. Smith Faculty of Agriculture, Food and Environment, The Hebrew University of Jerusalem, Rehovot 7610001, Israel
[5]Institute of Plant Sciences and Genetics in Agriculture, The Robert H. Smith Faculty of Agriculture, Food and Environment, The Hebrew University of Jerusalem, Rehovot 7610001, Israel
[6]Howard Hughes Medical Institute, The Salk Institute for Biological Studies, La Jolla, CA 92037, United States

* Corresponding author: ecker@salk.edu

Keywords: Stress Recovery, Drought Stress, Plant Immunity, Plant Genomics, Single-Cell.

Summary

All organisms experience stress as an inevitable part of life, from single-celled microorganisms to complex multicellular beings. The ability to recover from stress is a fundamental trait that determines the overall resilience of an organism, yet stress recovery is understudied. To begin unraveling the stress recovery process we studies recovery from drought stress in *Arabidopsis thaliana*. We performed a fine-scale time series of bulk RNA sequencing starting 15 minutes after rehydration following moderate drought. We reveal that drought recovery is a rapid process involving the activation of thousands of recovery-specific genes. To capture these rapid recovery responses in different leaf cell types, we performed single-nucleus transcriptome analysis at the onset of post-drought recovery, identifying a cell type-specific transcriptional state developing within 15 minutes of rehydration independently across cell types. Furthermore, we reveal a recovery-induced activation of the immune system that occurs independent of infection, which enhances pathogen resistance *in vivo* in *A. thaliana*, wild tomato (*Solanum pennellii)* and domesticated tomato (*Solanum lycopersicum* cv. M82). Since rehydration promotes microbial proliferation and thereby increases the risk of infection[1-2], drought recovery-induced immunity may be crucial for plant survival in natural environments. These findings indicate that drought recovery coincides with a preventive defense response, unraveling the complex regulatory mechanisms that facilitate stress recovery in different plant cell types.

35 **Main**

36 In most plants, extended periods of water deficit result in reduced growth, premature flowering,
37 flower abortion, fruit abscission, and, ultimately, decreased yield[3-4]. Plant responses to drought have
38 therefore been studied extensively as part of efforts to develop strategies or genetic manipulations that could
39 mitigate the economic and agricultural consequences of future droughts.

40 Previous studies have identified and functionally characterized numerous genes that respond to
41 water deficit, including various transcription factors (TFs) that regulate plant drought responses[4-6]. In
42 general, drought stress in plants induces dramatic changes in the transcriptional landscape[7-8]. For example,
43 the rapid up-regulation of genes involved in osmolyte accumulation enables water retention by adjusting
44 cellular osmotic potential[9]. However, efforts to enhance drought tolerance through genetic manipulation
45 have frequently resulted in undesired growth inhibition under non-drought conditions, thereby constraining
46 the widespread engineering and adoption of drought-resilient crops[6,10-11].

47 Given these limitations, we considered an alternative approach to investigating stress resilience in
48 plants by focusing on post-drought recovery rather than drought resistance. Indeed, understanding a plant's
49 ability to recover from drought is central to a comprehensive understanding of drought resilience, as the
50 potential for recovery defines whether the system can return to a stable state of function[12]. For example,
51 drought recovery has been established as an indicator of drought tolerance in annual crops such as maize[13-
52 14], wheat[15-16] and rice[17-18]. This extends to other abiotic stresses as well, for instance, the rates of
53 submergence recovery in *Arabidopsis thaliana* (Arabidopsis) accessions were found to correlate with their
54 submergence tolerance[19]. This finding suggests that the ability to recover after flooding is critical for plant
55 survival and reproductive success. One of the well-characterized plant responses to drought alleviation is
56 the downregulation of the drought responsive genes. For example, most drought-regulated genes recover to
57 normal expression levels within three hours of rehydration[20]. However, Oono et al.[21] identified 82
58 "recovery-specific" genes whose expression was drought-invariable but altered by subsequent rehydration.

59 Despite these known transcriptional responses during drought recovery, it remains unclear whether
60 these responses constitute a conserved drought recovery mechanism activated throughout the entirety of

61 plant cell types. Here, we explore the transcriptomic landscape in Arabidopsis throughout the drought
62 recovery process using a high-resolution time series of RNA sequencing data. We identified over 3,000
63 recovery-specific genes that were differentially expressed between 15 minutes and 6 hours after
64 rehydration. Using single-nucleus RNA-seq, we analyzed cell type-specific transcriptional signatures
65 immediately after inducing drought recovery. We identified a recovery unique transcriptional signature
66 common between sub-population of epidermal, hydathode, sieve element and mesophyll cells that is found
67 only once drought recovery is initiated. Within the gene modules enriched in sub-populations we found
68 many immune-associated genes. Based on these observations, we propose that some cells enter a recovery
69 cell state upon rehydration. The results indicated that one of the first steps of the recovery process is the
70 activation of a rapid preventive immune response. We therefore tested whether short-term recovery from
71 moderate drought activated functional immunity to block pathogen proliferation in plant leaves. In
72 agreement with this hypothesis, we found that drought recovery-induced activation of immune system
73 genes leads to reduced disease severity and bacterial load in infected leaves of both Arabidopsis and two
74 tomato species.

75 **Drought recovery-specific genes**

76 To study the transcriptional response to drought recovery, we performed a fine-scale RNA-seq time
77 series using vermiculite-grown Arabidopsis rosettes. We collected Arabidopsis rosettes during moderate
78 drought and at seven subsequent recovery time points within the six hours following rehydration (Fig. a-
79 b). At each time point, well-watered rosettes were also collected to control for diurnal transcriptional
80 changes (Fig. 1b). We then conducted a differential expression (DE) analysis of the treatments and time
81 points and defined two groups of genes: drought-responsive genes and recovery-specific genes. Drought-
82 responsive genes were defined as genes that were DE compared to well-watered plants during the drought
83 stress i.e., at time 0 (Extended Data Table 1). Conversely, recovery-specific genes were not DE during the
84 drought period but were DE in any of the post-drought recovery time points (Extended Data Table 2).

85 Based on these definitions, we identified 1,248 drought-responsive genes, of which 662 (53%) were
86 also DE during recovery. After only six hours of rehydration, 97% of these genes returned to normal
87 expression levels (Fig. 1c-d). We additionally identified over 3,000 recovery-specific genes across all
88 recovery time points (Fig. 1c and e), suggesting that drought recovery responses cannot be solely explained
89 by the alleviation of drought induced transcriptional responses. We used K-means clustering to characterize
90 gene expression patterns during drought and recovery. The drought-responsive genes exhibited five distinct
91 expression patterns (Fig. 1d): (1) drought-induced but downregulated during recovery, (2) drought-induced
92 but not DE during recovery, (3) drought- and recovery-induced; (4) drought-downregulated but recovery-
93 induced; and (5) drought-downregulated but not DE during recovery. Recovery-specific genes exhibited
94 three types of expression patterns based on whether they were induced in (1) early recovery or (2) late-
95 recovery or (3) downregulated by rehydration (Fig. 1e). These results demonstrate that drought recovery
96 involves the activation of thousands of recovery specific genes. These genes are timely regulated, with a
97 set of genes being upregulated from as early as 15 mins after rehydration, and a later set of genes starting
98 to accumulate after 30-60 mins.

99 **Global and cell type-specific recovery induced transcriptional reprogramming**

100 To create study the leaf cell type-specific transcriptional responses upon drought recovery, we
101 performed single-nucleus RNA-seq (snRNA-seq). For this experiment, we processed two replicates
102 undergoing long-term moderate drought and an additional two replicates after 15 minutes of rehydration,
103 as well as equivalent samples from well-watered controls. In this case, the well-watered controls were also
104 provided with 15 minutes of additional irrigation to ensure that any changes in gene expression were
105 specific to drought recovery and not due to mechanical root stress (Fig. 2a). After data quality control and
106 filtering, our integrated dataset included over 144,000 single-nuclei transcriptomes. The median number of
107 unique molecular identifiers (UMI) per nucleus was between 2,534 to 3,995 across the eight samples, and
108 the median number of genes detected per nucleus was between 1,213 to 1,698 (average 1,530; see Extended
109 Data Table 3).

110 Unsupervised clustering of the snRNA-seq profiles resulted in 27 clusters representing unique
111 molecular cell identities (Fig. 2b, Extended Data Figs. 1-2). All independent samples and treatment
112 conditions integrated into the same clusters (Extended Data Fig. 1). We used three major practices to
113 annotate cell identities for these clusters. First, we overlapped each cluster's marker genes (genes uniquely
114 or highly expressed in a certain cluster) with previously validated marker genes for all leaf cell types and
115 tissues (Extended Data Tables 4-5 and Extended Data Figs. 3-4). Second, we projected our dataset on
116 published single-cell datasets preformed on Arabidopsis leaves (Extended Data Fig. 5). Third, we manually
117 investigated the top marker genes in each cluster and used Gene Ontology (GO) enrichment analysis to see
118 enriched biological processes (Unknown clusters; Extended Data Fig. 6). Based on the genes expressed in
119 each cluster and their expression levels, we were able to confidently assign cell types to 22 of the 27 clusters.
120 Once the clusters had been assigned to cell types, we investigated cell type-specific changes during
121 the onset of drought recovery. A transcription factor (TF) expression analysis across the different treatments
122 revealed that TFs are rapidly induced by rehydration across all cell types. These TFs had many genes from
123 the *ETHYLENE RESPONSE FACTOR* (*ERF*) and *WRKY DNA-BINDING PROTEIN* (*WRKY*) families (Full
124 list in: Extended Data Table 6, GO term enrichment analysis in: Extended Data Fig. 7). In contrast, some
125 cell types, such as myrosin and vascular cells exhibited cell type-specific changes in TF expression upon
126 recovery. An interesting group of TFs were rapidly activated in a contextual manner that was both treatment
127 specific and cell state specific. These TFs were upregulated only in dividing cells at the onset of recovery
128 (Fig. 2d). Four gene families dominated this set of genes: MADS box, B3, NO APICAL MERISTEM
129 (NAC), and PAIRED AMPHIPATHIC HELIX (PAH2) families (Full list in: Extended Data Table 7).
130 Based on a sequence similarity analysis, the highly activated genes within each family were
131 phylogenetically clustered. For example, the upregulated MADS box genes were all type I MADS box (M-
132 type) genes: *AGAMOUS-LIKE43* (*AGL43*), *AGL89*, *AGL77*, *AGL75*, *AGL74*, *AGL84*, and *AGL50*.
133 Similarly, all the B3 TFs induced by drought recovery in dividing cells were in the REPRODUCTIVE
134 MERISTEM (REM) branch[22], despite the B3 family containing multiple distinct gene subfamilies[23]. These
135 findings suggest that drought recovery triggers cell type-specific transcriptional reprogramming.

136 **Recovery cell states in distinct cell types**

137 To study heterogeneity within cell types during drought recovery, we further subclustered cells
138 within each cell type based on their gene expression profiles (Extended Data Figs. 8-9). In epidermal,
139 mesophyll, hydathode, and sieve-element cells, some of the cell subpopulations were enriched (i.e., over
140 50% of cells in the subcluster) with cells from the drought recovery treated plants (Fig. 3a, Extended Data
141 Fig. 9). We hypothesized that these cell subpopulations form distinct subclusters due to their transition into
142 a recovery cell state (RcS). To test this hypothesis, we performed a motif enrichment analysis on each of
143 the suspected RcS subclusters to determine whether we could identify regulatory motifs that were common
144 to the putative RcS across all cell types. We found that all the subclusters that we identified as having an
145 activated RcS were enriched with the *CALMODULIN BINDING TRANSCRIPTION ACTIVATOR 1*
146 (*CAMTA1*) and *CAMTA5* binding motifs (Fig. 3b). In Arabidopsis, the CAMTA family of TFs regulate
147 plant defense and stress responses by modulating the expression of genes involved in pathogen defense,
148 abiotic stress tolerance, and plant development. These TFs interact with calcium-bound calmodulin to
149 mediate downstream signaling pathways[24]. To investigate if CAMTAs specifically regulate the RcS, we
150 performed motif enrichment analysis on all subclusters to see if the *CAMTA1* and *CAMTA5* motifs were
151 enriched in other subclusters. Out of 162 subclusters, only 9 subclusters were enriched with *CAMTA* motifs
152 (Extended Data Table 8, and Extended Data Fig. 10), suggesting that *CAMTA1* and *CAMTA5* are nearly
153 exclusively enriched in RcS subclusters, and could be the regulators of the formation of this cell state.

154 We predicted that *CAMTA1* and *CAMTA5* regulate the RcS; however, neither the CAMTA genes
155 nor the cell type-specific TFs predicted to regulate the RcS were upregulated in response to rehydration
156 (Fig. 3c). Since the RcS is rapidly activated, we hypothesized that *CAMTA* transcripts may be differentially
157 expressed during the early stages of drought and would therefore not be observed in our data, which was
158 collected after moderate drought had established. To test this hypothesis, we performed an additional
159 snRNA-seq experiment on Arabidopsis plants harvested each day over the course of five days starting from
160 the onset of drought (Fig. 3d, Extended Data Fig. 11). Cell identities were identified using unsupervised

161 clustering, as before. We then investigated the expression of *CAMTA* genes in different cell types during
162 early drought. In most cell types, *CAMTA* genes were upregulated in the days following dehydration (Fig.
163 3e, Extended Data Fig. 12), suggesting that the regulation of *CAMTA* is very sensitive to changes in water
164 availability and that *CAMTA* transcripts accumulate early in response to drought.

165 In addition to testing for a common regulatory pathway, we investigated whether the RcS
166 subpopulations within the different cell types expressed similar gene networks by performing gene co-
167 expression network analysis[25] for the seven cell clusters with an activated RcS subpopulation in the drought
168 recovery experiment (Fig. 3a). For each cluster, this analysis identified gene modules (Extended Data Fig.
169 13-14). We next searched for common hub genes (Genes with high module membership (kME) and high
170 intramodular connectivity (kIN)) among the modules that were enriched in RcS cells from different cell
171 types to identify genes that have common key roles in the formation of recovery cell states or its function.
172 Overall, we found 212 hub genes, of which 50 were shared by at least two modules (Extended Data Table
173 9). Interestingly, in the immediate recovery snRNAseq, 70% of the top marker genes for cluster "unknown
174 1" overlap with the hub genes identified in the RcS gene network. This finding led us to hypothesize that
175 cluster "unknown 1" represents a cell state that is superimposed across different cell types at the onset of
176 drought recovery (Extended Data Fig. 15).

177 Overall, the suite of common hub genes among the six RcS subclusters from different cell types
178 suggest that the functional onset of drought recovery in RcS subpopulations is comprised of cell wall
179 modifications and the regulation of nutrient uptake, as well as cytoplasmic detoxification processes and
180 DNA repair. The most prevalent hub genes shared among RcS subclusters are genes that play a critical role
181 in cell growth and plant development; these genes included *XYLOGLUCAN*
182 *ENDOTRANSGLUCOSYLASE/HYDROLASE 22* (*XTH22*)[26], *SLAC1 HOMOLOGUE 3* (*SLAH3*)[27], and
183 *EXORDIUM-LIKE1* (*EXL1*)[28]. Since toxins accumulate in plant cells during drought stress[29], we suspected
184 that detoxification may also be an important part of recovery. Indeed, our cross-cluster hub gene analysis
185 implicated *ARABIDOPSIS THALIANA DETOXIFICATION 1* (*AtDTX1*), which is localized in the plasma
186 membrane of plant cells and mediates the efflux of plant-derived or exogenous toxic compounds from the

187 cytoplasm[30]. An additional hub gene common across RcS cell populations was *CHROMATIN ASSEMBLY*
188 *FACTOR 1* (*CAF-1*) *AtCAF1a*, which facilitates the incorporation of histones H3 and H4 onto newly
189 synthesized DNA. The absence of the CAF-1 chaperone complex results in mitotic chromosome
190 abnormalities and changes in the expression profiles of genes involved in DNA repair[31]. In addition,
191 AtCAF1 proteins regulate mRNA deadenylation and defenses against pathogen infections[32]. Taken
192 together, these finding suggest that drought recovery triggers the formation of a specific cell state imposed
193 within several leaf cell types.

194 To identify more general processes involved in drought recovery, we performed a cell type-specific
195 differential expression analysis comparing plants harvested 15 minutes after the onset of drought recovery
196 to (i) plants experiencing drought and (ii) the well-watered controls that received additional irrigation for
197 15 min. Both controls were used for DE analysis to ensure that DE genes were not simply maintained from
198 their changes during drought or induced by the mechanical stress of additional watering. In nearly all cell
199 types, photosynthesis and carbon fixation were suppressed during the onset of drought recovery. The only
200 exception was in one of the seven mesophyll cell clusters, which maintained photosynthetic activity but
201 downregulated the expression of genes associated with bacterial responses (Extended Data Fig. 16a).
202 Conversely, genes that were upregulated at the onset of recovery were associated with diverse stressors
203 including wounding, cold, heat, light, and reactive oxygen species (i.e., oxidative stress). The upregulation
204 of such a broad suite of stress response genes suggests that the plant perceives the onset of recovery as a
205 state of stress, perhaps because recovery presents a change in the current homeostasis that was established
206 during drought.

207 **Recovery-induced immune responses**

208 We found evidence for the activation of multiple immunity-related genes in the top shared hub
209 genes among RcS subclusters. Among these genes for example, *TETRASPANIN 8* (*TET8*) has been shown
210 to be upregulated in response to the Flg22 and Elongation Factor Tu (EF-Tu) elicitors, which mimic
211 pathogen infection[33]. Another shared hub gene *SALT-INDUCIBLE ZINC FINGER 1* (*SZF1*) also regulates

212 plant immunity, as *szf1,2* knock-out mutants show increased susceptibility to *Pseudomonas syringae* pv.
213 *tomato* DC3000 (*Pst* DC3000)[34]. Three other shared hub genes (*AT5G41750, AT5G41740* and *AT4G19520*)
214 encode TOLL INTERLEUKIN RECEPTOR (TIR)–type NB-LRR proteins and thus belong to the most
215 common class of disease resistance genes in plants[35]. Another example is *ACTIVATED DISEASE*
216 *RESISTANCE 2* (*ADR2*) that enhances resistance to biotrophic pathogens[36]. Finally, we also found *EARLY*
217 *RESPONSIVE TO DEHYDRATION 15* (*ERD15*) as a top shared hub genes within the RcS enriched
218 modules, which belongs to a small and highly conserved protein family that is ubiquitous but specific to
219 the plant kingdom. Overexpression of ERD15 proteins in response to various pathogen elicitors was shown
220 to improve resistance to known pathogens and has also been shown to impair drought tolerance[37]. Thus, the
221 activation of a gene such as *ERD15* specifically upon rehydration maybe beneficial to contribute to plant
222 defense without compromising the drought response.

223 Other genes upregulated during the recovery initiation were implicated in processes associated with
224 plant immunity, including genes involved in response to bacterial pathogens, immune system processes,
225 responses to jasmonic acid (JA), and cell death. We found additional processes associated with plant
226 defense that were upregulated in specific cell types; for example, genes involved in the responses to
227 oomycetes or ethylene response were upregulated in almost all cell types during recovery, whereas defense
228 responses against insects were only upregulated in one-third of epidermal cell clusters, 50% of vascular cell
229 clusters, and two of the "unknown" clusters (Extended Data Fig. 16b).

230 We suspected that the transcriptomic upregulation of immune system processes during drought
231 recovery is an innate response to post-drought rehydration rather than a proactive response to microbial
232 infection following rehydration. To test this hypothesis, we examined the upregulation of recovery induced
233 genes under axenic conditions. Arabidopsis seedlings were grown on sterile agar plates for 14 days and
234 then transferred to low-water-content agar plates[38], which we produced by decreasing the water content of
235 the media to 50% (thus imposing moderate osmotic stress) (Extended Data Fig. 17a-b). After 14 days on
236 the low-water-content plates, plants were rehydrated and collected at different recovery time points (0, 15,
237 30, 90 and 120 min) for bulk RNA-seq analysis. The upregulation of the known drought marker genes

238 *RESPONSIVE TO DESICCATION 29A (RD29A), RD20*, and *DELTA1-PYRROLINE-5-CARBOXYLATE*
239 *SYNTHASE 1 (P5CS)*[39-41] confirmed that the plants were experiencing moderate drought stress (Extended
240 Data Fig. 17c). We additionally found that immune-related genes were upregulated after 15 minutes of
241 rehydration even in the axenic system (Extended Data Fig. 17d). These results support the hypothesis that
242 plants activate a prophylactic defense response upon recovery from moderate drought, independent of
243 pathogens in their environment.

244 Given the strength of this immunity-related transcriptional response during drought recovery, we
245 used data from Bjornson et al.[42] to evaluate how the genes implicated in our analysis correlated with known
246 transcriptional responses to biotic elicitors. Bjornson et al.[42] performed transcriptomic analysis across a
247 fine-scale time series to study rapid signaling transcriptional outputs induced by well-characterized elicitors
248 of pattern-triggered-immunity (PTI) in Arabidopsis. Their results showed that the transcriptional responses
249 to diverse microbial- or plant-derived molecular patterns are highly conserved. When we aligned these
250 identified transcriptional responses with the recovery specific genes identified by the bulk RNA-seq data
251 from the first two hours of our drought recovery time series (Fig. 1), we found that 50% of recovery-specific
252 genes upregulated after 15 minutes of rehydration overlap with the core responses to biotic elicitors in the
253 Bjornson et al.[42] dataset. More generally, this analysis shows a rapid and robust peak of immune-relevant
254 gene expression that gradually decreased with time since rehydration (Fig. 4a).

255 **Drought recovery-induced immunity *in vivo***

256 To test the functionality of post-recovery immune activation, we examined whether the activation
257 of immunity-related genes during short-term recovery from moderate drought promotes pathogen resistance
258 *in vivo*. We used the sterile low-water-content plate system and examined recovery from both moderate
259 (40% water-content) and severe stress (25% water-content), as described above. Plants from the control
260 and moderate or severe osmotic stress conditions were rehydrated for 90 minutes and then inoculated with
261 *Pst* DC3000 via submersion in a bacterial suspension. Whole rosettes were collected and weighed 48 hours
262 following infection and used to quantify bacterial growth. Plants recovering from drought had significantly

263 lower bacterial concentrations than control plants, and recovery from moderate stress suppressed bacterial
264 growth better than recovery from severe stress (Fig. 4b-c). These results suggest that recovery from
265 moderate drought enhances resistance to *Pst* DC3000.

266 To further validate these results, we grew plants on soil (non-sterile conditions) for 30 days under
267 short-day conditions. Drought-treated plants were transferred to dry trays and dehydrated for one week
268 down to 30% relative soil water content, while control plants continued to receive regular irrigation. We
269 rehydrated drought-treated plants for 90 minutes and then sprayed the leaves of both control and recovered
270 plants with *Pst* DC3000. Leaf discs were collected from each treatment 4 and 24 hours after inoculation,
271 surface sterilized, and then used to measure bacterial load. The bacterial load 4 hours after inoculation did
272 not differ between well-watered and drought-recovered plants. However, 24 hours after inoculation, the
273 bacterial load of drought-recovered plants was significantly lower than that of controls, indicating increased
274 resistance to *Pst* DC3000 in rehydrated plants (Fig. 4d-e). We call this response, which was consistent
275 across our two separate empirical tests, drought recovery-induced immunity (DRII).

276 Given the consistency of the DRII response in Arabidopsis, we further tested whether DRII is
277 conserved among various plant species and in response to different pathogens. First, we examined pathogen
278 proliferation in wild tomato plants recovering from moderate drought and infected with either *Pst* DC3000
279 or an additional tomato pathogen *Xanthomonas perforans* strain 97-2, which causes the tomato spot
280 disease[43]. For this test, we used the drought-tolerant tomato species *Solanum pennellii*[44]. We grew *S.*
281 *pennellii* plants at 25°C with a photoperiod of 12 hours light and 12 hours dark. When the plants had two
282 to three true leaves (~4 weeks old), we exposed them to moderate drought by stopping irrigation until the
283 soil reached 30% water content relative to saturated pots, as we had done for Arabidopsis. Drought was
284 then alleviated by irrigating pots to full saturation, and plants were infected 90 minutes after rehydration.
285 Both the drought-recovered plants and well-watered controls were syringe-infiltrated with a suspension of
286 either *X. perforans* 97-2 or *Pst* DC3000.

287 We first assessed disease severity in the well-watered and drought-recovered infected leaves by
288 imaging inoculated leaves 5 days post infection and calculating the percentage of symptomatic area relative

289 to the entire leaf surface. Leaves inoculated 90 minutes after recovery from moderate drought were
290 significantly less symptomatic than leaves from well-watered controls (Fig. 5a-b). To directly measure
291 bacterial concentrations in leaves, we compared leaf samples at an initial time point 4 hours after inoculation
292 to samples collected 5 days post-inoculation. Although a similar number of bacteria entered the leaves of
293 all plants, the plants that recovered from drought had a significantly lower bacterial load after five days
294 (Fig. 5c). Our results were consistent in both tested pathogens: regardless of the pathogen, tomato leaves
295 that recovered from drought exhibited lower disease severity and reduced bacterial concentrations than
296 control plants. Our observation that short-term recovery from moderate drought increases pathogen
297 resistance across all treatments further suggests that DRII is a preventive immune response that enhances
298 pathogen resistance during the initial period of drought recovery.

299 To further investigate DRII in an agriculturally relevant plant species, we repeated our post-drought
300 immune challenge experiment using a cultivar of domesticated tomato, *Solanum lycopersicum* cv. M82
301 (M82), and the same two pathogens as before (*Pst* DC3000 and *X. perforans* 97-2). Because breeders focus
302 on traits such as fruit size, shelf life, and brix, among others, we suspected that the DRII response could be
303 lost during domestication. However, M82 plants showed similar results to *S. pennellii* upon infection with
304 either pathogen (Fig. 6d-f), indicating that the DRII response we observed in Arabidopsis and *S. pennellii*
305 following short-term recovery from moderate drought is retained in domesticated tomato. We think that the
306 robustness of the DRII trait to the domestication processes underscores its potential significance in
307 agricultural contexts.

308 **Conclusion**

309 As large regions of the world gradually become drier, drought has become one of the most pressing
310 threats to global food security[45-46]. Plant drought responses have therefore been studied extensively over the
311 past decades, but the molecular mechanisms for drought recovery have been largely overlooked. We
312 advanced the understanding of drought recovery processes by using bulk RNA-seq over a six-hour time
313 series to identify recovery-specific genes. The resulting data enriches the pool of potential targets for

314 developing drought-tolerant crops. For example, the genes whose expression was drought-invariable but
315 downregulated during recovery ("cluster 3" in Fig. 1e) could be viable candidates for mutation screens
316 aimed at improving post-drought effects and recovery dynamics without affecting drought resistance.
317 Furthermore, the construction of a single-cell RNA-seq-based cell atlas of plants recovering from moderate
318 drought allowed us to explore cell type-specific transcriptional changes in response to drought and
319 immediate recovery. We were able to identify the major cell types in our dataset, and our findings suggest
320 that the five unidentified clusters (Fig. 2b) most likely contain multiple cell types that clustered together
321 because they were engaging in similar molecular or biochemical process during drought recovery, and
322 therefore cluster by the transcriptional signature of a specific cellular state. As plants must constantly adapt
323 to environmental changes, the molecular phenotypes of individual cells might vary to facilitate the
324 metabolic and biochemical changes essential for adaptation to the current stressor.

325 Using our drought recovery single cell atlas, we identified the first regulatory steps underlying the
326 transcriptional plasticity that allows plants to restore normal growth following drought. One of these steps
327 involves upregulating a set of TFs specifically in dividing cells within 15 minutes of rehydration. However,
328 little is known about the TFs identified by this analysis, although they largely belonged to four known TF
329 families—the MADS box, B3, NAC, and PAH2 families. The MADS box family of TFs are well known
330 for regulating flowering[47-48]. However, *AGL16* was shown to negatively regulate drought resistance via its
331 effects on stomata[49]. The B3 family members contains a highly conserved DNA-binding domain and are
332 involved in a variety of biological processes, many of which are related to the regulation of flowering
333 through polycomb silencing[50-52]. The NAC TFs play important roles in development as well as abiotic and
334 biotic stress responses[53]. Overall, the within-family phylogenetic proximity of the specific TFs upregulated
335 by recovery suggest that these TFs act together to play a functional role in drought recovery, though
336 determining the specific role of each TF will require further investigation of higher-order mutants.

337 Recently, Oliva et al.[55] characterized a highly active transcriptional state that affects a subset of
338 cells in different cell types across the developmental axis of the Arabidopsis root tip. The conserved cell
339 state was named environmentally responsive state (ERS), since many ERS enriched genes were previously

340 identified as responsive to various environmental cues. Here, we identified a transcriptional recovery cell
341 state (RcS) that is triggered by environmental stimuli. This state emerges in different cell types rapidly and
342 independently. We hypothesize that the RcS formation is governed by a small set of TFs, some of which
343 are common among cell types such as *CAMTA1* and *CAMTA5*. It is possible that some cell type-specific
344 TFs are also involved in the regulation of RcS depending on the cell type that the state was imposed on.

345 Our findings also show that transcripts for the calcium dependent *CAMTA* TFs accumulate during
346 early drought, and that, although the upregulation of *CAMTAs* does not persist during drought recovery,
347 many of the genes abundant during the RcS are regulated by *CAMTA1* and *CAMTA5*. Previous studies have
348 shown that calcium flux can be affected by changes in water availability (both water deficit and water
349 uptake)[54]. We therefore hypothesize that *CAMTA1 and CAMTA5* expression is induced during the early
350 stages of soil dehydration and that CAMTA proteins are post-translationally stabilized. CAMTAs activate
351 gene expression by interacting with calcium-bound calmodulin (CaM), and the influx of calcium upon
352 rehydration leads to an increase in calcium-bound calmodulin that then activates CAMTA proteins to bind
353 DNA and hence regulate the subsequent rehydration response. CaM levels may therefore be a limiting
354 factor in the regulation of the rapid CAMTA1-dependent gene activation that we observed in the initial
355 stages of drought recovery.

356 Our analysis suggest that the onset of drought recovery is coupled with the activation of a
357 preventive immune response. Plants have evolved complex defense networks in response to microbial
358 pathogens[35]. Aerial pathogens like *Pst* DC3000 or *X. perforans* mainly enter plants through stomatal pores,
359 but the stomata close in response to drought stress[56], making it harder for shoot pathogens to successfully
360 attack plants experiencing drought. It should be noted that some pathogenic bacteria have evolved specific
361 virulence factors to cause stomatal opening[57]. Moreover, plant immune responses can be sporadically
362 induced by the circadian clock even in the absence of a pathogenic threat, a process driven largely by daily
363 oscillations in humidity[58-59]. Such responses allow plants to prepare for the increased risk of infection when
364 microbes are anticipated to be most infectious. Because rehydration promotes both pathogen proliferation
365 and stomatal opening at a time when the immune system has already been suppressed by drought, plants

366 are particularly vulnerable to pathogen attack during the initial stages of drought recovery[60-61]. The rapid
367 upregulation of immunity genes that we observed in our study may therefore be crucial for ensuring plant
368 survival in water-fluctuating environments. We accordingly propose that DRII is a preventive immune
369 response that evolved to confer resistance against pathogens during drought recovery.

370 More broadly, our research shifts the focus from the well-studied drought responses to plant
371 transcriptional activity during the recovery period. Although plant responses to drought have been
372 extensively studied for over a century, these findings have yet to be successfully translated to the
373 development of drought-tolerant crops[62]. Our results highlight the presence and importance of recovery-
374 specific mechanisms that could be targeted in future experiments and engineering projects. We suggest a
375 new avenue for research in which efforts to improve crop resilience should focus not only on survival during
376 drought but also on rapid and effective recovery. By targeting recovery-specific genes, we can now
377 endeavor to develop crops that not only withstand drought but also recover more swiftly, ensuring minimal
378 yield loss and sustainable food production in an era of increasing climate unpredictability.

379 **Main references**

380 1. Palmero, D. *et al.* Fungal microbiota from rain water and pathogenicity of Fusarium species
381 isolated from atmospheric dust and rainfall dust. *J. Ind. Microbiol. Biotechnol.* **38**, 13–20 (2011).
382 2. Schwartz, H. F., Otto, K. L. & Gent, D. H. Relation of temperature and rainfall to development of
383 Xanthomonas and Pantoea leaf blights of onion in Colorado. *Plant Dis.* **87**, 11–14 (2003).
384 3. Campos, H., Cooper, M., Habben, J. E., Edmeades, G. O. & Schussler, J. R. Improving drought
385 tolerance in maize: A view from industry. *F. Crop. Res.* **90**, 19–34. (2004).
386 4. Bruce, W. B., Edmeades, G. O. & Barker, T. C. Molecular and physiological approaches to maize
387 improvement for drought tolerance. *J. Exp. Bot.* **53**, 13–25. (2002).
388 5. Singh, D. & Laxmi, A. Transcriptional regulation of drought response: A tortuous network of
389 transcriptional factors. *Front. Plant Sci.* **6**, 1–11. (2015).
390 6. Shim, J. S. *et al.* Overexpression of OsNAC14 improves drought tolerance in rice. *Front. Plant*
391 *Sci.* **9**, 1–14. (2018).
392 7. Shinozaki, K., Yamaguchi-Shinozaki, K. & Seki, M. Regulatory network of gene expression in
393 the drought and cold stress responses. *Curr. Opin. Plant Biol.* **6**, 410–417 (2003).
394 8. Soma, F., Takahashi, F., Yamaguchi-Shinozaki, K. & Shinozaki, K. Cellular phosphorylation
395 signaling and gene expression in drought stress responses: Aba-dependent and aba-independent
396 regulatory systems. *Plants* **10**, 1–16. (2021).
397 9. Zhang, J., Nguyen, H. T. & Blum, A. Genetic analysis of osmotic adjustment in crop plants. *J.*
398 *Exp. Bot.* **50**, 291–302. (1999).
399 10. Qin, F. *et al.* Regulation and functional analysis of *ZmDREB2A* in response to drought and heat
400 stresses in *Zea mays* L. **50**, 54–69. (2007).
401 11. Illouz-Eliaz, N. *et al.* Mutations in the tomato gibberellin receptors suppress xylem proliferation
402 and reduce water loss under water-deficit conditions. *J. Exp. Bot.* **71**, 3603–3612. (2020).
403 12. Gessler, A., Bottero, A., Marshall, J. & Arend, M. The way back: recovery of trees from drought
404 and its implication for acclimation. *New Phytol.* **228**, 1704–1709. (2020).
405 13. Hayano-Kanashiro, C., Calderón-Vázquez, C., Ibarra-Laclette, E., Herrera-Estrella, L. &
406 Simpson, J. Analysis of gene expression and physiological responses in three Mexican maize
407 landraces under drought stress and recovery irrigation. *PLoS One*. **4**(10), e7531. (2009).
408 14. Chen, D. *et al*. Genotypic variation in growth and physiological response to drought stress and re-
409 watering reveals the critical role of recovery in drought adaptation in maize seedlings. *Front*
410 *Plant Sci*. **6**(1241), 1-15. (2016).
411 15. Vassileva, V., Signarbieux, C., Anders, I. & Feller, U. Genotypic variation in drought stress
412 response and subsequent recovery of wheat (*Triticum aestivum L.*). *J Plant Res*. **124**(1), 147-154.
413 (2011).
414 16. Abid, M. *et al*. Adaptation to and recovery from drought stress at vegetative stages in wheat
415 (*Triticum aestivum*) cultivars. *Funct Plant Biol*. **43**(12), 1159-1169. (2016).
416 17. Kamoshita, A., Rodriguez, R., Yamauchi, A., & Wade, L. Genotypic variation in response of
417 rainfed lowland rice to prolonged drought and rewatering. *Plant Production Science*. **7**(4), 406-
418 420. (2004).
419 18. Efisue, A., Tongoona, P., Derera, J. & Ubi, B.E. Screening early generation progenies of
420 interspecific rice genotypes for drought stress tolerance during vegetative phase. *J Crop Improv*.
421 **23**, 174–193. (2009).
422 19. Yeung, E. *et al.* A stress recovery signaling network for enhanced flooding tolerance in
423 *Arabidopsis thaliana*. *Proc. Natl. Acad. Sci. U. S. A.* **115**, E6085–E6094 (2018).
424 20. Huang, D., Wu, W., Abrams, S. R. & Cutler, A. J. The relationship of drought-related gene
425 expression in *Arabidopsis thaliana* to hormonal and environmental factors. *J. Exp. Bot.* **59**,
426 (2008).
427 21. Oono, Y. *et al.* Monitoring expression profiles of Arabidopsis gene expression during rehydration
428 process after dehydration using ca. 7000 full-length cDNA microarray. *Plant J.* **34**, 868–887

429 (2003).
430 22. Romanel, E. A. C., Schrago, C. G., Couñago, R. M., Russo, C. A. M. & Alves-Ferreira, M.
431 Evolution of the B3 DNA binding superfamily: New insights into REM family gene
432 diversification. *PLoS One* **4**, (2009).
433 23. Wang, Y. *et al.* Systematic analysis of plant-specific B3 domain-containing proteins based on the
434 genome resources of 11 sequenced species. *Mol. Biol. Rep.* **39**, 6267–6282 (2012).
435 24. Iqbal, Z., Shariq Iqbal, M., Singh, S. P. & Buaboocha, T. Ca2+/Calmodulin Complex Triggers
436 CAMTA Transcriptional Machinery Under Stress in Plants: Signaling Cascade and Molecular
437 Regulation. *Front. Plant Sci.* **11**, 1–16 (2020).
438 25. Morabito, S., Reese, F., Rahimzadeh, N., Miyoshi, E. & Swarup, V. hdWGCNA identifies co-
439 expression networks in high-dimensional transcriptomics data. *Cell Rep Methods*. **3**(6), 100498.
440 (2023).
441 26. Xu, W. *et al.* Arabidopsis TCH4, regulated by hormones and the environment, encodes a
442 xyloglucan endotransglycosylase. *Plant Cell* **7**, 1555–1567 (1995).
443 27. Liu, B. *et al.* The anion channel SLAH3 interacts with potassium channels to regulate nitrogen-
444 potassium homeostasis and the membrane potential in Arabidopsis. *Plant Cell* **35**, 1259–1280
445 (2023).
446 28. Smith, A. M. & Stitt, M. Coordination of carbon supply and plant growth. *Plant, Cell Environ.*
447 **30**, 1126–1149 (2007).
448 29. Ahluwalia, O., Singh, P. C. & Bhatia, R. A review on drought stress in plants: Implications,
449 mitigation and the role of plant growth promoting rhizobacteria. *Resour. Environ. Sustain.* **5**,
450 6267-6282 (2021).
451 30. Li, L., He, Z., Pandey, G. K., Tsuchiya, T. & Luan, S. Functional cloning and characterization of
452 a plant efflux carrier for multidrug and heavy metal detoxification. *J. Biol. Chem.* **277**, 5360–
453 5368 (2002).
454 31. Varas, J., Santos, J. L. & Pradillo, M. The absence of the arabidopsis chaperone complex CAF-1
455 produces mitotic chromosome abnormalities and changes in the expression profiles of genes
456 involved in DNA repair. *Front. Plant Sci.* **8**, 1–11 (2017).
457 32. Liang, W. *et al.* The Arabidopsis homologs of CCR4-associated factor 1 show mRNA
458 deadenylation activity and play a role in plant defence responses. *Cell Res.* **19**, 307–316 (2009).
459 33. Wang, F. *et al.* Functional analysis of the Arabidopsis tetraspanin gene family in plant growth and
460 development. *Plant Physiol.* **169**, 2200–2214 (2015).
461 34. Kong, L. *et al.* Noncanonical mono(ADP-ribosyl)ation of zinc finger SZF proteins counteracts
462 ubiquitination for protein homeostasis in plant immunity. *Mol. Cell* **81**, 4591-4604.e8 (2021).
463 35. Jones, J.D.J., & Dangl, J.L. The plant immune system. *Nature* **444**, 323–329 (2006).
464 36. Aboul-Soud, M.A.M. *et al.* Activation tagging of ADR2 conveys a spreading lesion phenotype
465 and resistance to biotrophic pathogens. *New Phytol.* **183**, 1163–1175 (2009).
466 37. Kariola, T. *et al.* Early responsive to dehydration 15, a negative regulator of abscisic acid
467 responses in arabidopsis. *Plant Physiol.* **142**, 1559–1573 (2006).
468 38. Gonzalez, S. & Swift, J. *et al*. Arabidopsis transcriptome responses to low water potential using
469 high-throughput plate assays. *eLife*. **12**, RP84747 (2023).
470 39. Msanne, J., Lin, J., Stone, J. M. & Awada, T. Characterization of abiotic stress-responsive
471 *Arabidopsis thaliana* RD29A and RD29B genes and evaluation of transgenes. *Planta* **234**, 97–
472 107 (2011).
473 40. Aubert, Y. *et al.* RD20, a stress-inducible caleosin, participates in stomatal control, transpiration
474 and drought tolerance in *Arabidopsis thaliana*. *Plant Cell Physiol.* **51**, 1975–1987 (2010).
475 41. Székely, G. *et al.* Duplicated P5CS genes of Arabidopsis play distinct roles in stress regulation
476 and developmental control of proline biosynthesis. *Plant J.* **53**, 11–28 (2008).
477 42. Bjornson, M., Pimprikar, P., Nürnberger, T. & Zipfel, C. The transcriptional landscape of
478 *Arabidopsis thaliana* pattern-triggered immunity. *Nat. Plants.* **7**, 579–586 (2021).
479 43. Jones, J. B., Lacy, G. H., Bouzar, H., Stall, R. E. & Schaad, N. W. Reclassification of the

xanthomonas associated with bacterial spot disease of tomato and pepper. *Syst. Appl. Microbiol.* **27**, 755–762 (2004).

44. Bolger, A. *et al.* The genome of the stress-tolerant wild tomato species *Solanum pennellii*. *Nat. Genet.* **46**, 1034–1038 (2014).
45. Gupta, A., Rico-Medina, A. & Caño-Delgado, A. I. The physiology of plant responses to drought. *Science.* **368**, 266–269 (2020).
46. CRED. Climate in action Executive Summary. *EM-DAT | Int. disasters database* 8 (2022).
47. Pinyopich, A. *et al.* Assessing the redundancy of MADS-box genes during carpel and ovule development. *Nature* **424**, 85–88 (2003).
48. Callens, C., Tucker, M. R., Zhang, D. & Wilson, Z. A. Dissecting the role of MADS-box genes in monocot floral development and diversity. *J. Exp. Bot.* **69**, 2435–2459 (2018).
49. Zhao, P. X., Miao, Z. Q., Zhang, J., Chen, S. Y., Liu, Q. Q., & Xiang, C. B. Arabidopsis MADS-box factor AGL16 negatively regulates drought resistance via stomatal density and stomatal movement. *J. Exp. Bot*. **71**(19), 6092–6106 (2020).
50. Sung, S. & Amasino, R. M. Vernalization in *Arabidopsis thaliana* is mediated by the PHD finger protein VIN3. *Nature* **427**, 159–164 (2004).
51. Franco-Zorrilla, J. M. *et al.* AtREM1, a member of a new family of B3 domain-containing genes, is preferentially expressed in reproductive meristems. *Plant Physiol.* **128**, 418–427 (2002).
52. Levy, Y. Y., Mesnage, S., Mylne, J. S., Gendall, A. R. & Dean, C. Multiple roles of Arabidopsis VRN1 in vernalization and flowering time control. *Science.* **297**, 243–246 (2002).
53. Welner D.H., Deeba F., Lo Leggio L., Skriver K. Chapter 13—NAC Transcription Factors: From Structure to Function in Stress-Associated Networks. In: Gonzalez D.H., editor. *Plant Transcription Factors.* pp. 199–212. Academic Press; Boston, MA, USA. (2016).
54. Shao, H. B., Song, W. Y., & Chu, L. Y. Advances of calcium signals involved in plant anti-drought. *C. R. Biol.* **331** (8), 587–596. (2008).
55. Oliva, M. *et al*. An environmentally responsive transcriptional state modulates cell identities during root development. *bioRxiv* doi: https://doi.org/10.1101/2022.03.04.483008 (2022).
56. Cai, S. *et al.* Evolutionary Conservation of ABA Signaling for Stomatal Closure. *Plant Physiol.* **174**(2), 732-747. (2017).
57. Melotto, M. *et al*. Plant stomata function in innate immunity against bacterial invasion. *Cell.* **126**(5), 969-980. (2006).
58. Wang, W. *et al.* Timing of plant immune responses by a central circadian regulator. *Nature* **470**, 110–115 (2011).
59. Zhou, M. *et al.* Redox rhythm reinforces the circadian clock to gate immune response. *Nature* **523**, 472–476 (2015).
60. Palmero, D. *et al.* Fungal microbiota from rain water and pathogenicity of Fusarium species isolated from atmospheric dust and rainfall dust. *J. Ind. Microbiol. Biotechnol.* **38**, 13–20 (2011).
61. Schwartz, H. F., Otto, K. L. & Gent, D. H. Relation of temperature and rainfall to development of Xanthomonas and Pantoea leaf blights of onion in Colorado. *Plant Dis.* **87**, 11–14 (2003).
62. Dalal, A., Attia, Z. & Moshelion, M. To produce or to survive: How plastic is your crop stress physiology? *Front. Plant Sci.* **8**, 1–8 (2017).

521 **Figures**

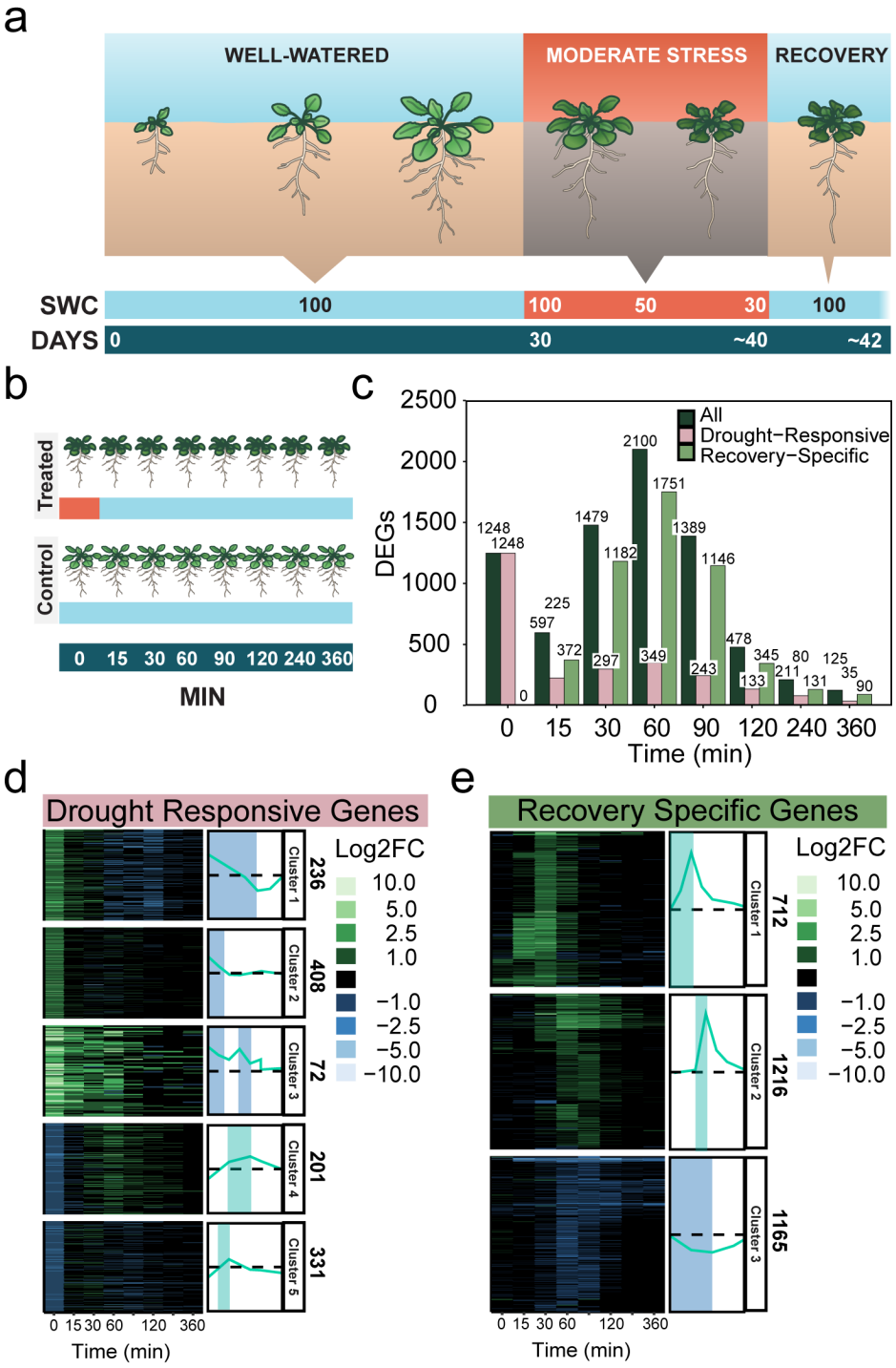

522 **Figure 1. A fine-scale RNA-seq time course of drought recovery reveals recovery-specific genes.**
523 **a,** Illustration of the recovery time-course experimental design. Plants were grown in vermiculite under a
524 short-day photoperiod. After 30 days, irrigation was stopped for drought-treated plants until they reached
525 30% relative soil water content (SWC). We then rehydrated the drought-treated plants by saturating the
526 vermiculite to initiate drought recovery. We collected 3 biological samples from each time point of
527 recovery, and well-watered control at each time point (n=3) **b,** Illustration of the samples collected for

528 RNA-seq. We collected samples during moderate drought (t=0 at 30% SWC) and at seven additional
529 time-points during the recovery process, from 15 min to six hours after rehydration. All samples from
530 drought-treated plants were collected alongside equivalent samples from well-watered controls, with three
531 replicates per treatment (drought or control) per time point. **c,** Number of differentially expressed genes
532 (DEGs) at different time points during recovery. For each time point, we show the total number of DEGs
533 as well as the numbers of drought-responsive and recovery-specific genes. DEGs were identified by
534 comparing drought-treated samples to well-watered controls at each time point. **d-e,** K-means clustering
535 and expression patterns of **d,** drought-responsive and **e,** recovery-specific genes.

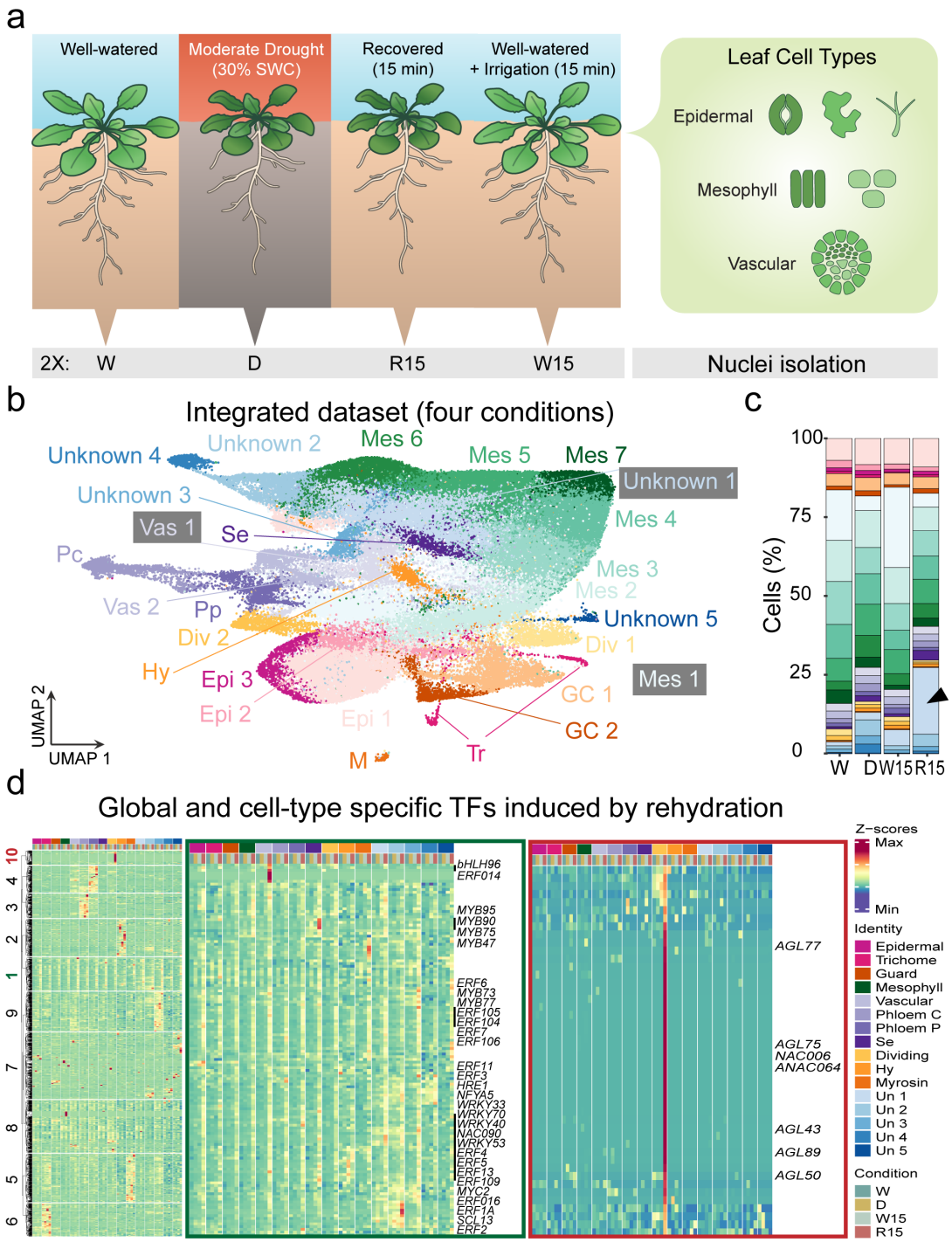

Figure 2. Drought recovery is initiated via transcriptional reprogramming in proliferating cells. **a,** Illustration of the experimental design used to generate a single-nucleus gene expression map. We collected two biological samples (n=2) from each of four conditions: (1) well-watered plants prior to drought [W]; (2) plants experiencing moderate drought [D]; (3) drought-treated plants after 15 min of rehydration [R15]; and (4) well-watered plants after 15 min of additional irrigation [W15]. **b,** Uniform Manifold Approximation and Projection (UMAP) of the integrated single-nucleus RNA-seq dataset revealed 27 cell identities encompassing the major leaf cell types: epidermal 1-3 (Epi), guard cell 1-2 (GC), trichome (Tr), hydathode (Hy), myrosin (M), mesophyll 1-7 (Mes), phloem parenchyma (Pp), phloem companion (Pc), sieve element (Se), and dividing 1-2

544 (Div). Five clusters could not be assigned to a cell type (Unknown 1-5). **c,** Cell identities recovered from each of
545 the four conditions, expressed as a percent of the total number of recovered cells. Plants experiencing drought
546 maintain similar cell identities, but the initiation of recovery leads to enrichment of one of the unidentified
547 clusters (Unknown 1). **d,** Gene expression of Arabidopsis TFs during drought and immediate recovery
548 represented by Z-score. In green square, cluster 1 genes, representing TFs globally induced by rehydration in
549 most cell types. In red square, cluster 10 genes that were strongly induced by rehydration, specifically in
550 dividing cells.

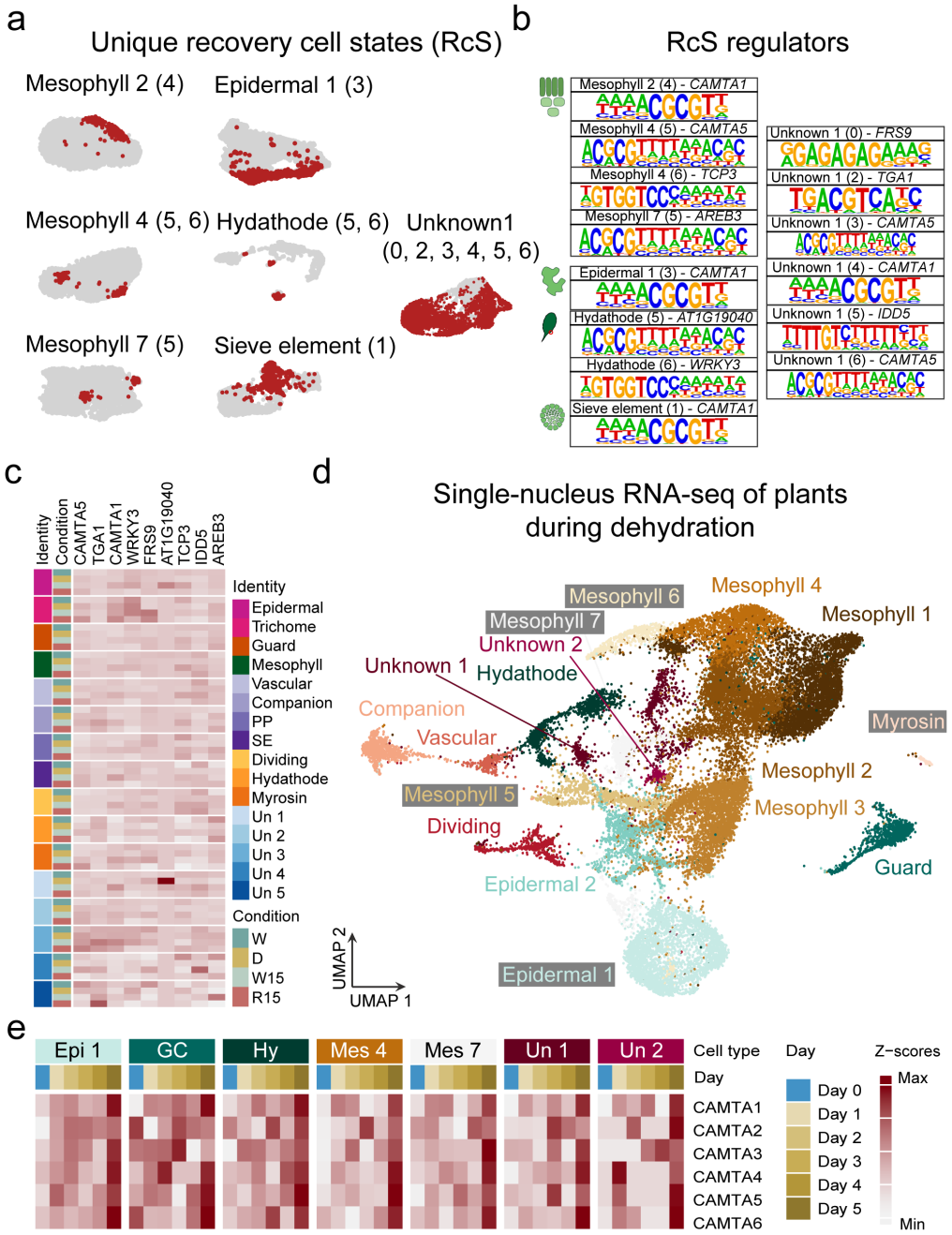

Figure 3. Recovery cell states (RcS) appear in sub-populations of epidermal, mesophyll, hydathode, and vascular cells. a, Subclustering of cells within each cell type from Fig. 2C revealed unique subclusters enriched in cells from plants recovering from drought. Drought-recovered cells are indicated in red. **b,** Putative regulators of the RcS, identified using *de novo* motif enrichment analysis performed for each recovery-enriched subcluster. The gene name above each motif is the predicted TF that binds the enriched motif. **c,** Z-score representation showing the expression levels of the TFs that putatively regulate the formation of the post-drought RcS. **d,** Uniform Manifold Projection and Approximation (UMAP) of the snRNA-seq data generated from *Arabidopsis* rosettes over the course of a five-day dehydration experiment. We collected multiple rosettes for each day and processed them as one biological replicate (n=1). **e,** Z-score representation showing the expression levels of predicted CAMTA TFs during the early stages of plant dehydration.

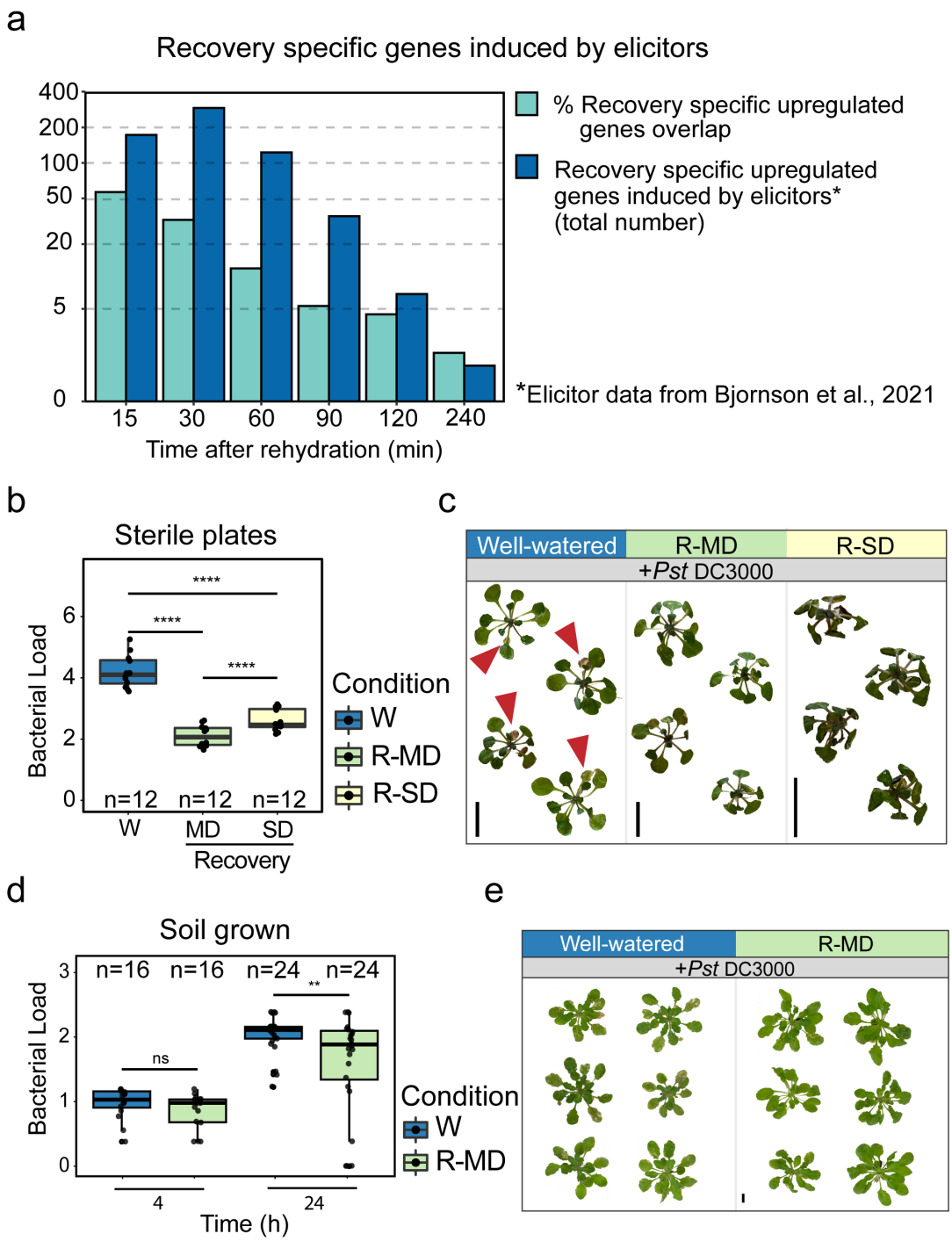

Figure 4. Recovery from moderate drought enhanced pathogen resistance in *Arabidopsis*. **a,** Overlap between upregulated recovery-specific genes in our bulk RNA-seq data and genes upregulated by different biotic elicitors as reported by Bjornson et al. (2021). For each recovery time point, bars show both the percentage of upregulated recovery-specific genes that are also known to be activated by biotic elicitors as well as the total number. **b,** Bacterial load ($\log_{10}$CFU) of plants that were grown on sterile low-water-content plates and then submerged in a suspension of *Pseduomonas syringae* pv. *tomato* DC3000 (*Pst* DC3000, OD_{600}=0.005) or a control solution. Bacterial growth was measured two days post-inoculation, and well-watered controls (W) were compared against plants recovering from either moderate (R-MD) or severe drought (R-SD). For this analysis, we merged two independent experiments for a total of n=12 per treatment. Significance values were calculated with a two-way ANOVA of treatment and batch followed by Tukey's *post hoc* test. P-values were FDR-corrected. **c,** Representative images of plants taken four days post-inoculation. **d,** Bacterial load ($\log_{10}$CFU)

572 of soil-grown plants sprayed with *Pst* DC3000 (OD_{600}=0.05) or a control solution after experiencing moderate
573 drought. Bacterial growth was measured 4 and 24 hours post-inoculation and compared against controls using a
574 two-way student's t-test. We collected 16 leaves (n=16) to measure bacterial load at the initial time point, and 24
575 leaves (n=24) to measure bacterial growth 24 hours post infection. **e,** Representative images of plants taken 14
576 days post-inoculation. In **b** and **d**: ns = $P > 0.05$, * = $P \leq 0.05$, ** = $P \leq 0.01$, *** = $P \leq 0.001$, **** = $P \leq$
577 0.0001. Boxplots middle line shows the median, the lower and upper hinges are the 25th and 75th percentile,
578 respectively. The whiskers extend from the hinges to the most distant value within 1.5 * IQR of the hinge, where
579 IQR is the inter-quartile range, or distance between the first and third quartiles.

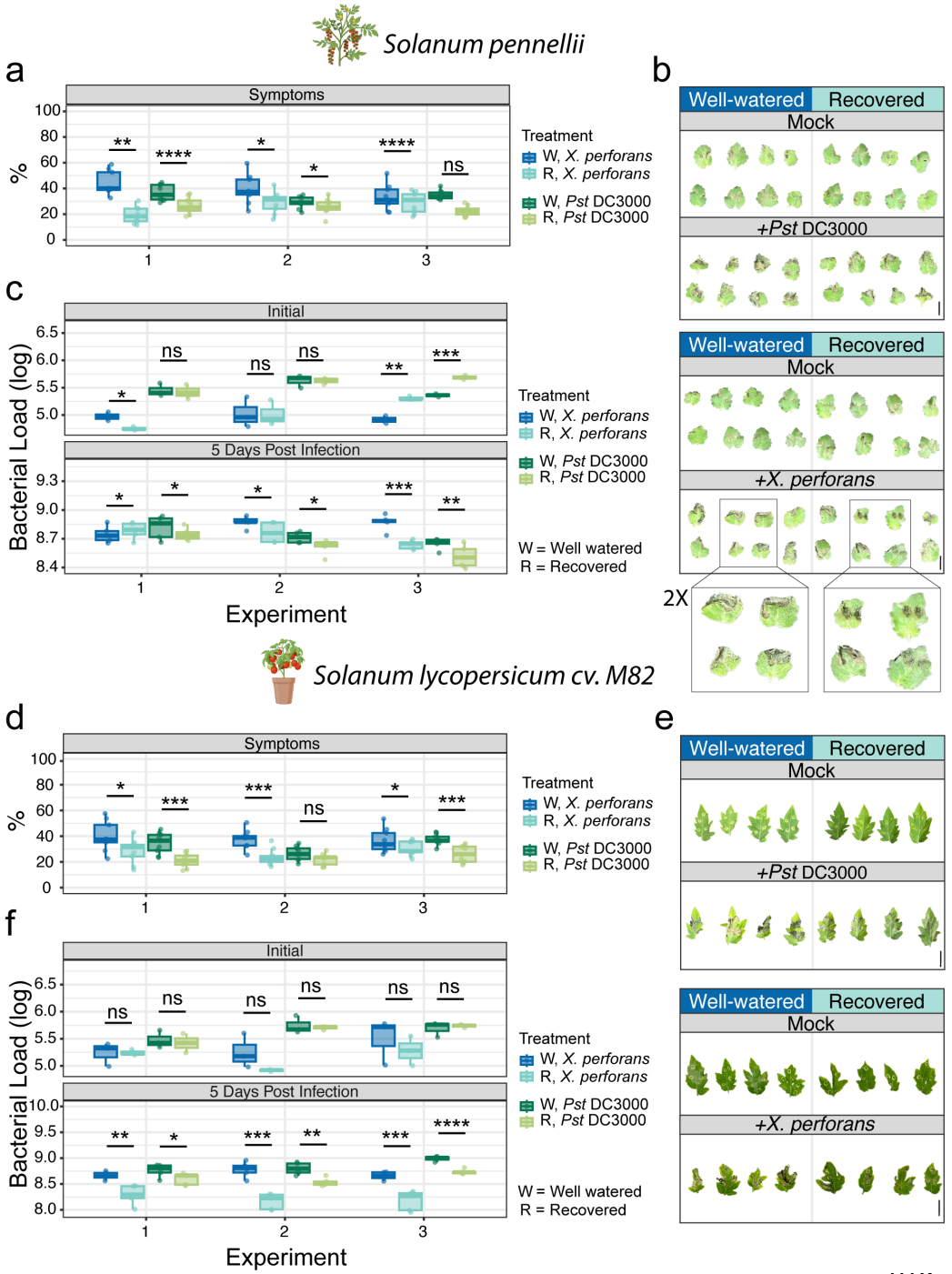

Figure 5. Drought recovery-induced immunity enhanced resistance to *X. perforans* and *Pst* DC3000 in wild (*Solanum pennellii*) and domesticated (*S. lycopersicum* cv. M82) tomato species. a, Lesion percentage analysis of *S. pennellii* leaves five days after being syringe infiltrated with either *X. perforans* OD_{600}= 0.02 or *Pst* DC3000 OD_{600}= 0.02. Inoculation was performed after 90 mins of recovery from moderate drought, and drought-treated samples were compared to well-watered controls. Results are shown for three independent experiments, 9 leaves were analyzed in each experiment (n=9). **b,** Representative images of well-watered or drought-recovered *S. pennellii* leaves infected with one of *Pst* DC3000, *X. perforans*, or a mock solution. Scale bar = 1 cm. **c,** Bacterial load (log_{10}CFU) of the *S. pennellii* leaves measured five days post-infection. Results are shown for three independent experiments. 2 leaf discs (0.5 cm in diameter) were prepared for each sample, 5 samples were used for each independent experiment (n=5). **d,** Lesion percentage analysis of M82 leaves after undergoing the same post-drought infection experiment described for *S. pennelli*. 9 leaves were analyzed in each

experiment (n=9). **e,** Representative images of M82 leaves infected with *Pst* DC3000, *X. perforans*, or a mock solution. Scale bar = 2 cm. **f,** Bacterial load (log_{10}CFU) of M82 leaves measured five days post-infection. Results are shown for three independent experiments. 2 leaf discs (0.5 cm in diameter) were prepared for each sample, 5 samples were used for each independent experiment (n=5). Significant differences in all panels were identified using student's t-test (ns = $P > 0.05$, * = $P \leq 0.05$, ** = $P \leq 0.01$, *** = $P \leq 0.001$, **** = $P \leq 0.0001$). Boxplots middle line shows the median, the lower and upper hinges are the 25th and 75th percentile, respectively. The whiskers extend from the hinges to the most distant value within 1.5 * IQR of the hinge, where IQR is the inter-quartile range, or distance between the first and third quartiles.

638 **Methods**

639 ***Plant materials and growth conditions***

640 *Arabidopsis thaliana* Columbia-0 (Col-0) background was used throughout this study. Col-0 seeds were
641 sterilized with chlorine fumes generated by mixing 100 ml bleach and 4 ml hydrochloric acid (HCl 1M). Sterilized
642 seeds were sown on large square petri dishes with ¾ Linsmaier & Skoog with buffer (LS) media per liter and 2%
643 agar, and then stratified at 4 °C for three days. Plates were placed in a growth chamber and grown in short-day
644 conditions (8h light: 16h dark) at 22 °C with a light intensity of ~110–130 μmol m^{-2} s^{-1}. For drought treatments,
645 seedlings were transferred to vermiculite pots two weeks after germination on plates, with 6 seedlings per pot.
646 Tray size was 27.79 cm width, 54.46 cm in length, and 6.2 cm depth. Vermiculite was saturated with ¾ LS liquid
647 media before the seedling transfer, 2L media per tray. After two days, each tray was watered with 2L ultra-pure
648 water, and this continued for two weeks until the drought treatment started. When plants were 30 days old, each
649 pot was weighed and transferred to a dry tray. The pots in the tray were weighed daily, and relative water content
650 was calculated. The experiment started when the pots reached 30% relative soil-water content (SWC). Three whole
651 Arabidopsis rosettes per treatment were collected separately as an independent sample, time 0 was 9 am (one hour
652 after the lights turn on in the chambers). Three samples per treatment were collected alongside a well-watered
653 control at each time point. For sterile low-water agar experiments, plates were prepared modified from Gonzales
654 et al., 2023; 100% - 4L DDW, 3 LS bags, 80g agar – 120ml per plate, 50% (moderate stress) - 2L DDW, 3 LS
655 bags, 80g agar – 60ml per plate, and 25% (severe stress) - 1L DDW, 3 LS bags, 80g agar – 30ml per plate.

656 For the drought time course experiment, plants were grown on plates and transferred to vermiculite as
657 described above with the notable exception that transfer from plates took place 17 days after germination and
658 remained on saturated vermiculite for 12 days before drought initiation. Drought was initiated by draining excess
659 media from the pot and equilibrating to 100% relative SWC. Whole rosettes (n= 3 – 6) were sampled and frozen
660 4.5 hours after subjective dawn each day for 5 days.

661 Col-0 seeds were sterilized and seeded on plates. Plates were kept in the dark at 4C for three days. After
662 three days, plates were moved to a growth chamber with short-day photoperiod light and 22 °C temperature.

663 Tomato seeds of *Solanum pennellii* and *Solanum lycopersicum* cv. M82 were germinated in a petri dish
664 with 1/2 Murashige & Skoog (MS) with vitamins and FeNaEDTA (Cat# 07190008) media (no sucrose added).

665 Ten-days-old seedlings were transferred to tray pots containing a mixture of vermiculite (Agrekal Moshav
666 Habonim) and commercial soil (Tuff A.C.S) (1:1 by volume) and grown in a 12-hour light-dark cycle (12h light:
667 12h dark) at 25°C.

668 ***Bacterial inoculation***

669 *Pseudomonas syringae* pv. *tomato (Pst)* DC3000 was grown overnight in 10 ml liquid King's B medium
670 containing rifampicin (40 µg/ml) (Cat#: R3501-250MG, MilliporeSigma, MA) and tetracyclin (10 mg/ml) (Cat#:
671 T3258, MilliporeSigma, MA) at 28°C for 24 h. Before adjusting the density, bacterial cells were washed two times
672 with autoclaved water followed by centrifugation at 6,000 rpm for 2 min and re-suspension in water. For bacterial
673 growth assays, well-watered and 90 min recovered Arabidopsis plants were inoculated with *Pst* DC3000 (OD_{600}
674 = 0.005-0.5, depending on the experiment and inoculation method). For spray treatment Silwett77 (Cat#: S7777,
675 PhytoTachLabs, KS) was added to bacteria before spraying. Bacterial titer was assessed as the $\log_{10}$ transformed
676 colony forming units (CFU) per plant weight when collecting whole plants from sterile plates.

677 For experiments performed on tomato, syringe infiltration was used for bacterial inoculation. For
678 bacterium counting, ten leaf discs (0.5 cm in diameter) were prepared from the second and third true leaves using
679 a hole puncher (two discs per leaf) for each sample, five samples were used for each independent experiment. Each
680 sample was separately homogenized in 10 mM $MgCl_2$. The homogenate was serially diluted in 10 mM $MgCl_2$.
681 10µl of diluted homogenate were plated on antibiotics and LB agar media on a square petri dish and incubated at
682 28°C for 48 h for determination of bacterial concentrations in leaves ($\log^{10}$ CFU/cm^2).

683 ***Assessment of disease severity in in tomato leaves***

684 Disease severity in tomato (*S. pennellii* and *S. lycopersicum* cv. M82) leaves was assessed by calculating
685 the percentage of the symptomatic area in the leaves relative to the whole leaf area. The calculation was done
686 based on threshold color and color space HSB in ImageJ version 1.54d, according to Tuang et al.[1] Nine leaves per
687 experiment were analyzed for the lesion percentage (%).

688 ***RNA extraction, bulk RNA library construction***

689 Total RNA was extracted from three independent biological replicates of each time point using RNeasy
690 Plant Mini Kits (Cat#79254, Qiagen, CA). Tape Station checked RNA quantity for quality control. Library
691 construction was performed using Illumina Stranded mRNA Prep (Cat#20040534, Illumina, CA).

692 ***Nuclei extraction and single-nuclei library construction***

693 Seedlings were transferred to vermiculite pots two weeks after germination in trays, 6 seedlings per pot.
694 Vermiculite was saturated with ¾ LS liquid media before the seedling transfer, 2L media per tray. After two days
695 each tray was watered with 2L ultra-pure water, and this continued for two weeks until the drought treatment
696 started. When plants were 30 days old, each pot was weighed and transferred to a dry tray. The experiment began
697 when each pot reached 30% SWC. Between 12-18 whole rosettes were collected for each time point * condition
698 sample. We used mortar and pestle to grind the frozen tissue. Powdered tissue was then placed in a nuclei extraction
699 buffer [NEB; 500ul 1M TRIS pH=7.4 (Cat# 15567027, Thermo Fisher Scientific, MA), 150µl 1M $MgCl_2$ (Cat#
700 AM9530G, Fisher Scientific, MA), 100µl 1M NaCl (Cat# AM9760G Fisher Scientific, MA), 50ml nuclease-free
701 water (Cat# AM9937 Thermo Fisher Scientific, MA), 25µl 1M spermine (Cat# 85590-5G, MilliporeSigma, MA),
702 10µl 1M spermidine (Cat# S2626-5G, MilliporeSigma, MA), 500µl proteinase inhibitor (PI; Cat# P9599-5ML
703 MilliporeSigma, MA), 250µl BSA (Cat# B2518-100MG, MilliporeSigma, MA), 250µl SUPERase-In (Cat#
704 AM2696, Thermo Fisher Scientific, MA)] and incubated for 10 min. After incubation, tissue was filtered through
705 a 40µm filter (Cat# 43-57040-51, pluriSelect, Germany). We then centrifuged at 500 rcf for 5 min at 4°C.
706 Supernatant was aspirated out, and nuclei were resuspended with NEB + 500µl 10% Triton (Cat# 93443-100ML,
707 MilliporeSigma, MA) and no PI. We incubated for 15 min, filtered through a 40µm filter, and spun at 500 rcf for
708 5 min. We washed until the pellet was clear. We prepared the density gradient using the Density Buffer [DB; 120
709 mM Tris-Cl pH=8 (Cat# AM9855G, Fisher Scientific, MA), 150 mM KCl (Cat# AM9640G, Fisher Scientific,
710 MA), 30 mM MgCl2, 35mL H_20 per 50mL] and filter sterilized it. We mixed 5 volumes of Optiprep (Cat# D1556-
711 250ML, MilliporeSigma, MA) and the buffer volume to create a 50% stock. We also made a dilutant stock [400
712 mM Sucrose, 25 mM KCl, 5 mM $MgCl_2$, 10 mM Tris-Cl pH 8, 28mL H_20 per 50mL] that we filter sterilized. A
713 45% solution was made by mixing 9ml 50% solution and 1ml dilutant, and a 15% solution by combining 1.5ml

714 50% stock and 3.5ml dilutant. We created a 45% solution and a 15% solution. We gently poured 2ml of the nuclei
715 solution at the top of the density gradient and then spun the tubes at 1,500 rcf for 5 min with no breaks. After the
716 spin, we pipette off nuclei and place them into a 15 ml tube with ~ 6mL of NEB (with no triton or PI). We note
717 that for vermiculite drought stressed nuclei, nuclei preparations were FACS purified. After counting the nuclei,
718 the nuclei suspension was loaded onto microfluidic chips (10X Genomics) with HT-v3.1 chemistry to capture
719 ~20,000 nuclei/sample. Cells were barcoded with a Chromium X Controller (10X Genomics). mRNA was reverse
720 transcribed, and Illumina libraries were constructed for sequencing with reagents from a 3' Gene Expression HT-
721 v3.1 kit (10X Genomics) according to the manufacturer's instructions. cDNA and final library quality were
722 assessed using Tape-Station High Sensitivity DNA Chip (Agilent, CA).
723 Each of the single-nuclei samples was processed twice, to get a higher number of single nuclei
724 transcriptomes.

725 ***Bulk RNA-sequencing and analysis***

726 Sequencing was performed with a NovaSeq 6000 instrument (Illumina, CA). About 40 million reads were
727 obtained for each sample. Raw reads were processed at the IGC bioinformatics core at Salk. Alignments were
728 performed using OSA4 and mapped to the Arabidopsis genome (TAIR 10) using Tophat2 software with default
729 settings. Mapped reads per library were counted using HTSeq software. Differentially expressed genes were
730 quantified in two ways. Firstly, differentially expressed genes were identified using a spline regression model in
731 splineTimeR v1.18.0, which were then sorted into time points using k-means clustering. Differential expression
732 was also quantified at each time point individually using DESeq2 v1.30.0.[2] For each pairwise comparison, genes
733 with fewer than 32 total raw counts across all samples were discarded before normalization. Genes with an absolute
734 $\log_2$foldchange > 1 and an FDR-corrected p-value ≤ 0.01 were pulled as significant. For functional enrichment,
735 genes were queried for time-specific functional enrichment using over-representation analysis (ORA) in
736 WebGestaltR v0.4.4.[3] Differentially expressed genes in each pairwise comparison were queried against the
737 biological process non-redundant ontology, and a significance threshold of FDR-corrected p-value ≤ 0.05 was
738 used.

739 ***snRNA-seq analysis***

740 For the snRNA-seq libraries, CellRanger (v.6.0.1) was used to perform sample-demultiplexing, barcode
741 processing, and single-nuclei gene-UMI counting.[4] Each experiment's expression matrix was obtained by aligning
742 to Arabidopsis transcriptome reference (TAIR 10) using CellRanger with default parameters. For initial quality-
743 control filtering, aligned cell and transcript counts from each treatment (well-watered, drought, recovery, 2
744 replicates each) were processed by Seurat (Version 4.2).[5] The data was filtered in the following two ways: (1) Pre-
745 filtering each replicate by removing the low-quality and outlier cells containing a high abundance of chloroplast
746 reads (>40% of total transcripts) and mitochondrial reads (>1% of total transcripts), a low abundance of detected
747 genes (<300 detected genes) and a relatively high abundance of unique molecular identifiers (UMIs) (>10K for
748 D0; >15K and >10K for two W15, respectively; >25K and >20K for two W0 , respectively; >10K for R15)
749 (Extended Data Table 3). (2) Identifying possible doublet in each replicate using the method SCDS. SCDS
750 implements two complementary approaches to identify doublets: one is co-expression-based doublet scoring, and
751 the other is binary classification-based doublet scoring. Additionally, they provide a hybrid score by combing these
752 two approaches. SCDS showed relatively high detection accuracy and computational efficiency when
753 benchmarking with other computational methods.[6] We applied the hybrid scores for doublet estimation using R
754 package scds() to identify likely doublet and then removed them from downstream integration. Expression data of
755 cells passing these thresholds were log normalized with NormalizeData() function, and the top2K variable genes
756 were identified with the FindVariableFeatures() function. Next, data from all conditions were integrated using
757 Seurat's reciprocal PCA (RPCA) and FindIntegrationAnchors() functions to identify integration features and
758 correct for potential batch effects. The integrated data were then scaled with ScaleData() function. Principal
759 component analysis (PCA) was carried out with RunPCA() function, and the top 30 principal components (PCs)
760 were retained. Clusters were identified with the FindClusters() function using the shared nearest neighbor
761 modularity optimization with a clustering resolution set to 0.8. Clusters with only one cell were removed. This
762 resulted in 27 initial clusters with a total of 144,494 cells. We identified a median number of 1,500 genes, and
763 3,146 UMIs (representing unique transcripts), per nuclei. We detected between 25,064 – 26,342 genes in each

764 sample. Cell-type identity of initial clusters was determined with canonical markers and by referring to public
765 datasets, followed by sub-clustering each cluster using the same strategy described above.

766 Single cell differential gene expression analysis was conducted using Seurat FindMarker() and
767 FindAllmarkers() functions with the default Wilcoxon Rank Sum test. Marker genes per cell cluster and
768 differentially expressed genes (DEGs) among conditions were both identified by setting parameter min.pct as 0.1
769 and picked the top expressed markers ranking by average $\log_2$FC. Functional enrichment analysis was carried out
770 by over-representation analysis (ORA) using the top100 markers ranked by average $\log_2$FC. Using the GO
771 biological process as a reference, ORA was performed with WebGestalt.[3] Pathways with FDR <0.05 were
772 considered significantly enriched and visualized as plots with normalized enrichment scores. For recovery-
773 /drought-specific DEGs, enriched known motifs were discovered with HOMER findmotifs.pl
774 (http://homer.ucsd.edu/homer/), searching within 1000bp upstream to 1000kb downstream of their transcript start
775 sites (TSSs). For the sub-clusters, recovery-enriched cell clusters were identified with >=50% cells from recovery
776 experiment, followed with weighted gene co-expression network analysis (WGCNA) with R package hdWGCNA
777 (https://smorabit.github.io/hdWGCNA/). Co-expression networks were constructed for each initial cell cluster
778 with top 20 hub genes. By checking the average expression of hub genes in sub-clusters, the recovery-specific
779 networks were picked as those with higher expression in recovery-enriched cell clusters.

780 ***Statistical analysis***

781 bulk RNA-seq data, statistical analysis was performed in R using a mixed linear model function (lmer)
782 from the package lme4 unless otherwise described. Standard errors were calculated from variance and covariance
783 values after model fitting. The Benjamini-Hochberg method was applied for correcting of multiple testing in
784 figures showing all pairwise comparisons of the mean estimates. For bacterial colonies count, merged two
785 independent experiments of plants grown on plates, a total of n=12 per treatment. Significance values
786 for log10(CFU) on the plates were calculated with a two-way ANOVA of treatment and batch followed by a Tukey
787 test. P-values are FDR-corrected. For bacterial colonies count, soil grown plants experiment, significance values
788 for log10(CFU) were calculated with a two-way student's t-test.

789 ***Data availability***

790 Data is available here: GSE220278 (https://www.ncbi.nlm.nih.gov/geo/query/acc.cgi?acc=GSE220278).

791 Currently open only for reviewers.

792 ***Code availability***

793 The code used to analyze both bulk and single-nuclei RNA-Seq data is available at:

794 https://github.com/NatanellaIE/DroughtRecovery.

795 **Methods references**

796 1. Tuang, Z. K. *et al.* Pst DC3000 infection alleviates subsequent freezing and heat injury to host plants via
797 a salicylic acid-dependent pathway in Arabidopsis. *Plant Cell Environ.* **43**, 801–817 (2020).
798 2. Love, M. I., Huber, W. & Anders, S. Moderated estimation of fold change and dispersion for RNA-seq
799 data with DESeq2. *Genome Biol.* **15**, 1–21 (2014).
800 3. Liao, Y., Wang, J., Jaehnig, E. J., Shi, Z. & Zhang, B. WebGestalt 2019: gene set analysis toolkit with
801 revamped UIs and APIs. *Nucleic Acids Res.* **47**, 199–205 (2019).
802 4. Zheng, G. X. Y. *et al.* Massively parallel digital transcriptional profiling of single cells. *Nat. Commun.* **8**,
803 (2017).
804 5. Hao, Y. *et al.* Integrated analysis of multimodal single-cell data. *Cell* **184**, 3573-3587.e29 (2021).
805 6. Xi, N. M. & Li, J. J. Benchmarking Computational Doublet-Detection Methods for Single-Cell RNA
806 Sequencing Data. *Cell Syst.* **12**, 176-194 (2021).

807 **Extended data references**

808

809 1. Abe, M., Takahashi, T. & Komeda, Y. Cloning and characterization of an L1 layer-specific gene in
810 Arabidopsis thaliana. *Plant Cell Physiol.* **40**, 571–580 (1999).
811 2. Abe, M., Takahashi, T. & Komeda, Y. Identification of a cis-regulatory element for L1 layer-specific
812 gene expression, which is targeted by an L1-specific homeodomain protein. *Plant J.* **26**, 487–494 (2001).
813 3. Alvarez-Buylla, E. R. *et al.* MADS-box gene evolution beyond flowers: Expression in pollen, endosperm,
814 guard cells, roots and trichomes. *Plant J.* **24**, 457–466 (2000).
815 4. Baima, S. *et al.* The expression of the Athb-8 homeobox gene is restricted to provascular cells in
816 Arabidopsis thaliana. *Development* **121**, 4171–4182 (1995).
817 5. Kang, J. & Dengler, N. Vein pattern development in adult leaves of Arabidopsis thaliana. *Int. J. Plant*
818 *Sci.* **165**, 231–242 (2004).
819 6. Scarpella, E., Francis, P. & Berleth, T. Stage-specific markers define early steps of procambium
820 development in Arabidopsis leaves and correlate termination of vein formation with mesophyll
821 differentiation. *Development* **131**, 3445–3455 (2004).
822 7. Kim, J. Y. *et al.* Distinct identities of leaf phloem cells revealed by single cell transcriptomics. *Plant Cell*
823 **33**, 511–530 (2021).
824 8. Barth, C. & Jander, G. Arabidopsis myrosinases TGG1 and TGG2 have redundant function in
825 glucosinolate breakdown and insect defense. *Plant J.* **46**, 549–562 (2006).
826 9. Bonke, M., Thitamadee, S., Mähönen, A. P., Hauser, M. T. & Helariutta, Y. APL regulates vascular
827 tissue identity in Arabidopsis. *Nature* **426**, 181–186 (2003).
828 10. Truernit, E. & Sauer, N. The promoter of the Arabidopsis thaliana SUC2 sucrose-H+ symporter gene

829 directs expression of β-glucuronidase to the phloem: Evidence for phloem loading and unloading by
830 SUC2. *Planta An Int. J. Plant Biol.* **196**, 564–570 (1995).
831 11. Bulankova, P., Akimcheva, S., Fellner, N. & Riha, K. Identification of Arabidopsis meiotic cyclins
832 reveals functional diversification among plant cyclin genes. *PLoS Genet.* **9**(5), e1003508 (2013).
833 12. Chauvin, A., Caldelari, D., Wolfender, J. L. & Farmer, E. E. Four 13-lipoxygenases contribute to rapid
834 jasmonate synthesis in wounded Arabidopsis thaliana leaves: A role for lipoxygenase 6 in responses to
835 long-distance wound signals. *New Phytol.* **197**, 566–575 (2013).
836 13. Nguyen, C. T., Kurenda, A., Stolz, S., Chételat, A. & Farmer, E. E. Identification of cell populations
837 necessary for leaf-to-leaf electrical signaling in a wounded plant. *Proc. Natl. Acad. Sci. U. S. A.* **115**,
838 10178–10183 (2018).
839 14. Chen, L. Q. *et al.* Sucrose efflux mediated by SWEET proteins as a key step for phloem transport.
840 *Science.* **335**, 207–211 (2012).
841 15. Cui, H., Kong, D., Liu, X. & Hao, Y. SCARECROW, SCR-LIKE 23 and SHORT-ROOT control bundle
842 sheath cell fate and function in Arabidopsis thaliana. *Plant J.* **78**, 319–327 (2014).
843 16. De Rybel, B. *et al.* A bHLH complex controls embryonic vascular tissue establishment and indeterminate
844 growth in Arabidopsis. *Dev. Cell* **24**, 426–437 (2013).
845 17. Endo, M., Shimizu, H., Nohales, M. A., Araki, T. & Kay, S. A. Tissue-specific clocks in Arabidopsis
846 show asymmetric coupling. *Nature* **515**, 419–422 (2014).
847 18. Fisher, K. & Turner, S. PXY, a receptor-like kinase essential for maintaining polarity during plant
848 vascular-tissue development. *Curr. Biol.* **17**, 1061–1066 (2007).
849 19. Funk, V., Kositsup, B., Zhao, C. & Beers, E. P. The Arabidopsis xylem peptidase XCP1 is a tracheary
850 element vacuolar protein that may be a papain ortholog. *Plant Physiol.* **128**, 84–94 (2002).
851 20. Glaring, M. A. *et al.* An extra-plastidial α-glucan, water dikinase from Arabidopsis phosphorylates
852 amylopectin in vitro and is not necessary for transient starch degradation. *J. Exp. Bot.* **58**, 3949–3960
853 (2007).
854 21. Gotor, C., Cejudo, F. J., Barroso, C. & Vega, J. M. Tissue-specific expression of ATCYS-3A, a gene
855 encoding the cytosolic isoform of O-acetylserine(thiol)lyase in Arabidopsis. *Plant J.* **11**, 347–352 (1997).
856 22. Guo, W. J., Bundithya, W. & Goldsbrough, P. B. Characterization of the Arabidopsis metallothionein
857 gene family: Tissue-specific expression and induction during senescence and in response to copper. *New*
858 *Phytol.* **159**, 369–381 (2003).
859 23. Hsu, P. K. & Tsay, Y. F. Two phloem nitrate transporters, NRT1.11 and NRT1.12, are important for
860 redistributing xylem-borne nitrate to enhance plant growth. *Plant Physiol.* **163**, 844–856 (2013).
861 24. Kondo, T. *et al.* Stomatal density is controlled by a mesophyll-derived signaling molecule. *Plant Cell*
862 *Physiol.* **51**, 1–8 (2010).
863 25. Sugano, S. S. *et al.* Stomagen positively regulates stomatal density in Arabidopsis. *Nature* **463**, 241–244
864 (2010).
865 26. Lopez-Anido, C. B. *et al.* Single-cell resolution of lineage trajectories in the Arabidopsis stomatal lineage
866 and developing leaf. *Dev. Cell* **56**, 1043-1055 (2021).
867 27. Johnson, C. S., Kolevski, B. & Smyth, D. R. Transparent Testa Glabra2, a trichome and seed coat
868 development gene of arabidopsis, encodes a WRKY transcription factor. *Plant Cell* **14**, 1359–1375
869 (2002).
870 28. Kang, B. H., Busse, J. S. & Bednarek, S. Y. Members of the arabidopsis dynamin-like gene family,
871 ADL1, are essential for plant cytokinesis and polarized cell growth. *Plant Cell* **15**, 899–913 (2003).
872 29. Kasahara, R. D., Portereiko, M. F., Sandaklie-Nikolova, L., Rabiger, D. S. & Drews, G. N. MYB98 is
873 required for pollen tube guidance and synergid cell differentiation in Arabidopsis. *Plant Cell* **17**, 2981–
874 2992 (2005).
875 30. Wenzel, C. L., Schuetz, M., Yu, Q. & Mattsson, J. Dynamics of MONOPTEROS and PIN-FORMED1
876 expression during leaf vein pattern formation in Arabidopsis thaliana. *Plant J.* **49**, 387–398 (2007).
877 31. Jammes, F. *et al.* MAP kinases MPK9 and MPK12 are preferentially expressed in guard cells and
878 positively regulate ROS-mediated ABA signaling. *Proc. Natl. Acad. Sci. U. S. A.* **106**, 20520–20525
879 (2009).
880 32. Ji, J. *et al.* Wox4 promotes procambial development. *Plant Physiol.* **152**, 1346–1356 (2010).
881 33. Zhang, T. Q., Chen, Y. & Wang, J. W. A single-cell analysis of the Arabidopsis vegetative shoot apex.

882 *Dev. Cell* **56**, 1056-1074.e8 (2021).
883 34. Procko, C. *et al.* Leaf cell-specific and single-cell transcriptional profiling reveals a role for the palisade
884 layer in UV light protection. *Plant Cell* **34**, 3261–3279 (2022).
885 35. Kirschner, S. *et al.* Expression of SULTR2;2, encoding a low-affinity sulphur transporter, in the
886 Arabidopsis bundle sheath and vein cells is mediated by a positive regulator. *J. Exp. Bot.* **69**, 4897–4906
887 (2018).
888 36. Kurata, T. *et al.* The YORE-YORE gene regulates multiple aspects of epidermal cell differentiation in
889 Arabidopsis. *Plant J.* **36**, 55–66 (2003).
890 37. Mathur, J. *et al.* Transcription of the Arabidopsis CPD gene, encoding a steroidogenic cytochrome P450,
891 is negatively controlled by brassinosteroids. *Plant J.* **14**, 593–602 (1998).
892 38. Müller, R., Borghi, L., Kwiatkowska, D., Laufs, P. & Simon, R. Dynamic and compensatory responses of
893 Arabidopsis shoot and floral to meristems to CLV3 signaling. *Plant Cell* **18**, 1188–1198 (2006).
894 39. Chen, L. Q. *et al.* Sugar transporters for intercellular exchange and nutrition of pathogens. *Nature* **468**,
895 527–532 (2010).
896 40. Mustroph, A. *et al.* Profiling translatomes of discrete cell populations resolves altered cellular priorities
897 during hypoxia in Arabidopsis. *Proc. Natl. Acad. Sci. U. S. A.* **106**, 18843–18848 (2009).
898 41. Zhang, L. *et al.* Altered xylem-phloem transfer of amino acids affects metabolism and leads to increased
899 seed yield and oil content in Arabidopsis. *Plant Cell* **22**, 3603–3620 (2010).
900 42. Ohashi-Ito, K. & Bergmann, D. C. Arabidopsis FAMA controls the final proliferation/differentiation
901 switch during stomatal development. *Plant Cell* **18**, 2493–2505 (2006).
902 43. Okumoto, S. *et al.* High affinity amino acid transporters specifically expressed in xylem parenchyma and
903 developing seeds of Arabidopsis. *J. Biol. Chem.* **277**, 45338–45346 (2002).
904 44. Pilot, G. *et al.* Overexpression of GLUTAMINE DUMPER1 leads to hypersecretion of glutamine from
905 hydathodes of arabidopsis leaves. *Plant Cell* **16**, 1827–1840 (2004).
906 45. Pommerrenig, B. *et al.* Phloem-Specific expression of Yang cycle genes and identification of novel Yang
907 cycle enzymes in Plantago and Arabidopsis. *Plant Cell* **23**, 1904–1919 (2011).
908 46. Qiu, J. L., Jilk, R., Marks, M. D. & Szymanski, D. B. The Arabidopsis SPIKE1 gene is required for
909 normal cell shape control and tissue development. *Plant Cell* **14**, 101–118 (2002).
910 47. Susek, R. E., Ausubel, F. M. & Chory, J. Signal transduction mutants of arabidopsis uncouple nuclear
911 CAB and RBCS gene expression from chloroplast development. *Cell* **74**, 787–799 (1993).
912 48. Ranjan, A., Fiene, G., Fackendahl, P. & Hoecker, U. The Arabidopsis repressor of light signaling SPA1
913 acts in the phloem to regulate seedling de-etiolation, leaf expansion and flowering time. *Development*
914 **138**, 1851–1862 (2011).
915 49. Stadler, R. & Sauer, N. The Arabidopsis thaliana AtSUC2 gene is specifically expressed in companion
916 cells. *Bot. Acta* **109**, 299–306 (1996).
917 50. Rouse, D. T., Marotta, R. & Parish, R. W. Promoter and expression studies on an Arabidopsis thaliana
918 dehydrin gene. *FEBS Lett.* **381**, 252–256 (1996).
919 51. Zimmermann, I., Saedler, R., Mutondo, M. & Hulskamp, M. The Arabidopsis GNARLED gene encodes
920 the NAP125 homolog and controls several actin-based cell shape changes. *Mol. Genet. Genomics* **272**,
921 290–296 (2004).
922 52. Zhu, Y., Liu, L., Shen, L. & Yu, H. NaKR1 regulates long-distance movement of FLOWERING LOCUS
923 T in Arabidopsis. *Nat. Plants* **2**, (2016).
924 53. Zhang, X., Dyachok, J., Krishnakumar, S., Smith, L. G. & Oppenheimer, D. G. IRREGULAR
925 TRICHOME BRANCH1 in arabidopsis encodes a plant homolog of the actin-related protein2/3 complex
926 activator Scar/WAVE that regulates actin and microtubule organization. *Plant Cell* **17**, 2314–2326
927 (2005).
928 54. Yoshimoto, N., Inoue, E., Saito, K., Yamaya, T. & Takahashi, H. Phloem-localizing sulfate transporter,
929 Sultr1;3, mediates re-distribution of sulfur from source to sink organs in arabidopsis. *Plant Physiol.* **131**,
930 1511–1517 (2003).
931 55. Yephremov, A., *et al*. Characterization of the FIDDLEHEAD gene of Arabidopsis reveals a link between
932 adhesion response and cell differentiation in the epidermis. *Plant cell*, **11**(11), 2187–2201. (1999).
933 56. Xu, W. *et al.* Arabidopsis TCH4, regulated by hormones and the environment, encodes a xyloglucan
934 endotransglycosylase. *Plant Cell* **7**, 1555–1567 (1995).

57. Wu, H. *et al.* Molecular and biochemical characterization of the Fe(III) chelate reductase gene family in Arabidopsis thaliana. *Plant Cell Physiol.* **46**, 1505–1514 (2005).
58. Werner, T. *et al.* Cytokinin-deficient transgenic Arabidopsis plants show multiple developmental alterations indicating opposite functions of cytokinins in the regulation of shoot and root meristem activity. *Plant Cell* **15**(11), 2532–2550 (2003).
59. Uemoto, K., Araki, T. & Endo, M. Isolation of arabidopsis palisade and spongy mesophyll cells. *Methods Mol. Biol.* **1830**, 141–148 (2018).
60. Takemiya, A. *et al.* Phosphorylation of BLUS1 kinase by phototropins is a primary step in stomatal opening. *Nat. Commun.* **4**, 2094. (2013).
61. Takada, S., Takada, N. & Yoshida, A. ATML1 promotes epidermal cell differentiation in Arabidopsis shoots. *Dev.* **140**, 1919–1923 (2013).
62. Szymanski, D. B., Jilk, R. A., Pollock, S. M. & Marks, M. D. Control of GL2 expression in Arabidopsis leaves and trichomes. *Development* **125**, 1161–1171 (1998).
63. Zhang, F., Gonzalez, A., Zhao, M., Payne, C. T. & Lloyd, A. A network of redundant bHLH proteins functions in all TTG1-dependent pathways of Arabidopsis. *Development* **130**, 4859–4869 (2003).
64. Xia, Y., Nikolau, B. J. & Schnable, P. S. Developmental and hormonal regulation of the Arabidopsis CER2 gene that codes for a nuclear-localized protein required for the normal accumulation of cuticular waxes. *Plant Physiol.* **115**, 925–937 (1997).
65. Wallner, E. S. *et al.* Strigolactone- and Karrikin-Independent SMXL Proteins Are Central Regulators of Phloem Formation. *Curr. Biol.* **27**(8), 1241–1247 (2017).
66. Walker, A. R. *et al.* The TRANSPARENT TESTA GLABRA1 locus, which regulates trichome differentiation and anthocyanin biosynthesis in arabidopsis, encodes a WD40 repeat protein. *Plant Cell* **11**, 1337–1349 (1999).
67. Vanzin, G. F. *et al.* The mur2 mutant of Arabidopsis thaliana lacks fucosylated xyloglucan because of a lesion in fucosyltransferase AtFUT1. *Proc. Natl. Acad. Sci. U. S. A.* **99**, 3340–3345 (2002).
68. Van Leene, J. *et al.* Targeted interactomics reveals a complex core cell cycle machinery in Arabidopsis thaliana. *Mol. Syst. Biol.* **6**, (2010).
69. Vahisalu, T. *et al.* SLAC1 is required for plant guard cell S-type anion channel. *Nature* **452**, 487–491 (2008).
70. Takahashi, K. *et al.* Ectopic expression of an esterase, which is a candidate for the unidentified plant cutinase, causes cuticular defects in arabidopsis thaliana. *Plant Cell Physiol.* **51**, 123–131 (2010).
71. Ohashi, Y., Oka, A., Ruberti, I., Morelli, G. & Aoyama, T. Entopically additive expression of GLABRA2 alters the frequency and spacing of trichome initiation. *Plant J.* **29**, 359–369 (2002).
72. Swaminathan, K., Yang, Y., Grotz, N., Campisi, L. & Jack, T. An enhancer trap line associated with a D-class cyclin gene in Arabidopsis. *Plant Physiol.* **124**, 1658–1667 (2000).
73. Sistrunk, M. L., Antosiewicz, D. M., Purugganan, M. M. & Braam, J. Arabidopsis TCH3 encodes a novel Ca2+ binding protein and shows environmentally induced and tissue-specific regulation. *Plant Cell* **6**, 1553–1565 (1994).
74. Sinlapadech, T., Stout, J., Ruegger, M. O., Deak, M. & Chapple, C. The hyper-fluorescent trichome phenotype of the brt1 mutant of Arabidopsis is the result of a defect in a sinapic acid:UDPG glucosyltransferase. *Plant J.* **49**, 655–668 (2007).
75. Schlereth, A. *et al.* MONOPTEROS controls embryonic root initiation by regulating a mobile transcription factor. *Nature* **464**, 913–916 (2010).
76. Schellmann, S. *et al.* TRIPTYCHON and CAPRICE mediate lateral inhibition during trichome and root hair patterning in Arabidopsis. *EMBO J.* **21**, 5036–5046 (2002).
77. Sawchuk, M. G., Donner, T. J., Head, P. & Scarpella, E. Unique and overlapping expression patterns among members of photosynthesis-associated nuclear gene families in Arabidopsis. *Plant Physiol.* **148**, 1908–1924 (2008).
78. Sawa, S. *et al.* The HAT2 gene, a member of the HD-Zip gene family, isolated as an auxin inducible gene by DNA microarray screening, affects auxin response in Arabidopsis. *Plant J.* **32**, 1011–1022 (2002).
79. Saedler, R., Zimmermann, I., Mutondo, M. & Hülskamp, M. The Arabidopsis KLUNKER gene controls cell shape changes and encodes the AtSRA1 homolog. *Plant Mol. Biol.* **56**, 775–782 (2004).
80. Endo, M., Mochizuki, N., Suzuki, T. & Nagatani, A. CRYPTOCHROME2 in vascular bundles regulates

988 flowering in Arabidopsis. *Plant Cell* **19**, 84–93 (2007).
989 81. Redovniković, I. R., Textor, S., Lisnić, B. & Gershenzon, J. Expression pattern of the glucosinolate side
990 chain biosynthetic genes MAM1 and MAM3 of Arabidopsis thaliana in different organs and
991 developmental stages. *Plant Physiol. Biochem.* **53**, 77–83 (2012).
992 82. Pilot, G., Gaymard, F., Mouline, K., Chérel, I. & Sentenac, H. Regulated expression of Arabidopsis
993 Shaker K+ channel genes involved in K+ uptake and distribution in the plant. *Plant Mol. Biol.* **51**, 773–
994 787 (2003).
995 83. Oppenheimer, D. G. *et al.* Essential role of a kinesin-like protein in Arabidopsis trichome morphogenesis.
996 *Proc. Natl. Acad. Sci. U. S. A.* **94**, 6261–6266 (1997).
997 84. Kirik, V. *et al.* Ectopic expression of the Arabidopsis AtMYB23 gene induces differentiation of trichome
998 cells. *Dev. Biol.* **235**, 366–377 (2001).
999 85. Dinkeloo, K., Boyd, S. & Pilot, G. Update on amino acid transporter functions and on possible amino
1000 acid sensing mechanisms in plants. *Semin. Cell Dev. Biol.* **74**, 105–113 (2018).
1001 86. Negi, J. *et al.* A dof transcription factor, SCAP1, is essential for the development of functional stomata in
1002 arabidopsis. *Curr. Biol.* **23**, 479–484 (2013).
1003 87. Geisler, M., Nadeau, J. & Sack, F. D. Oriented asymmetric divisions that generate the stomatal spacing
1004 pattern in arabidopsis are disrupted by the too many mouths mutation. *Plant Cell* **12**, 2075–2086 (2000).
1005 88. Weichert, A. *et al.* AtPTR4 and AtPTR6 are differentially expressed, tonoplast-localized members of the
1006 peptide transporter/nitrate transporter 1 (PTR/NRT1) family. *Planta* **235**, 311–323 (2012).
1007 89. Schachtman, D. P. *et al.* Expression of an inward-rectifying potassium channel by the Arabidopsis KAT1
1008 cDNA. *Science (New York, N.Y.).* **258**, 5088 (1992).
1009 90. Menges, M. & Murray, J. A. H. Synchronous Arabidopsis suspension cultures for analysis of cell-cycle
1010 gene activity. *Plant J.* **30**, 203–212 (2002).
1011 91. Mayer, K F et al. Role of WUSCHEL in regulating stem cell fate in the Arabidopsis shoot meristem.
1012 *Cell*. **95**(6), 805-815. (1998).
1013 92. MacAlister, C. A., Ohashi-Ito, K. & Bergmann, D. C. Transcription factor control of asymmetric cell
1014 divisions that establish the stomatal lineage. *Nature* **445**, 537–540 (2007).
1015 93. Pillitteri, L. J., Sloan, D. B., Bogenschutz, N. L. & Torii, K. U. Termination of asymmetric cell division
1016 and differentiation of stomata. *Nature* **445**, 501–505 (2007).
1017 94. Schuster, J., Knill, T., Reichelt, M., Gershenzon, J. & Binder, S. BRANCHED-CHAIN
1018 AMINOTRANSFERASE4 is part of the chain elongation pathway in the biosynthesis of methionine-
1019 derived glucosinolates in Arabidopsis. *Plant Cell* **18**, 2664–2679 (2006).
1020 95. Lu, L., Lee, Y. R. J., Pan, R., Maloof, J. N. & Liu, B. An internal motor kinesin is associated with the
1021 golgi apparatus and plays a role in trichome morphogenesis in Arabidopsis. *Mol. Biol. Cell* **16**, 811–823
1022 (2005).
1023 96. Li, S. F., Higginson, T. & Parish, R. W. A novel MYB-related gene from Arabidopsis thaliana expressed
1024 in developing anthers. *Plant Cell Physiol.* **40**, 343–347 (1999).
1025 97. Lai, L. B. *et al.* The Arabidopsis R2R3 MYB proteins FOUR LIPS and MYB88 restrict divisions late in
1026 the stomatal cell lineage. *Plant Cell* **17**, 2754–2767 (2005).
1027 98. Kubo, M. *et al.* Transcription switches for protoxylem and metaxylem vessel formation. *Genes Dev*.
1028 **19**(16), 1855-1860. (2005)
1029 99. Kirik, V. *et al.* Functional diversification of MYB23 and GL1 genes in trichome morphogenesis and
1030 initiation. *Development* **132**, 1477–1485 (2005).
1031 100. O'Malley, R. C. *et al*. Cistrome and epicistrome features shape the regulatory DNA landscape.
1032 *Cell.* **165(**5), 1280-1292. (2016).
1033 101. Bar-Peled, M. & O'Neill, M. A. Plant nucleotide sugar formation, interconversion, and salvage by
1034 sugar recycling. *Annu Rev Plant Biol*. **62**,127-155. (2011).
1035 102. Lalonde, S., Wipf, D. & Frommer, W. B. Transport mechanisms for organic forms of carbon and
1036 nitrogen between source and sink. *Annu Rev Plant Biol*. **55**, 341-372. (2004).
1037 103. Cobbett, C. & Goldsbrough, P. Phytochelatins and metallothioneins: roles in heavy metal
1038 detoxification and homeostasis. *Annu Rev Plant Biol*. **53**, 159-182. (2002).

Acknowledgments

We want to thank T. Nolan for insightful comments to this manuscript. This research was supported by a Postdoctoral Award No. FI-601-2020 from the United States–Israel Binational Agricultural Research and Development Fund. N.I.-E. is a research fellow at the George E. Hewitt Foundation for Medical Research and an Awardee of the Weizmann Institute of Science – Israel National Postdoctoral Award Program for Advancing Women in Science and the Women's Postdoctoral Career Development Award. J.R.E. is an Investigator of the Howard Hughes Medical Institute.

Author contributions

Conceptualization – N.I-E
Data curation – N.I-E, R.G-C, J.S, B.J, T.Z-K, A.Y
Formal analysis – N.I-E, K.L, J.Y, J.R.N, T.Z-K
Funding acquisition - N.I-E, J.R.E
Investigation - N.I-E, R.G-C
Methodology - N.I-E, T.L, J.S, S.B, Y.Z
Project administration - N.I-E
Resources – J.R.E
Writing – original draft - N.I-E, J.R.E.

Declaration of interests

The authors declare no competing interests.